Non-Coherent UWB Communication in the Presence of Multiple Narrowband Interferers

Alberto Rabbachin, *Member, IEEE*, Tony Q.S. Quek, *Member, IEEE*, Pedro C. Pinto, *Student Member, IEEE*, Ian Oppermann, *Senior Member, IEEE*, and Moe Z. Win, *Fellow, IEEE*

***Abstract*—There has been an emerging interest in non-coherent ultra-wide bandwidth (UWB) communications, particularly for low-data rate applications because of its low-complexity and low-power consumption. However, the presence of narrowband (NB) interference severely degrades the communication performance since the energy of the interfering signals is also collected by the receiver. In this paper, we compare the performance of two non-coherent UWB receiver structures – the autocorrelation receiver (AcR) and the energy detection receiver (EDR) – in terms of the bit error probability (BEP). The AcR is based on the transmitted reference signaling with binary pulse amplitude modulation, while the EDR is based on the binary pulse position modulation. We analyze the BEPs for these two non-coherent systems in a multipath fading channel, both in the absence and presence of NB interference. We consider two cases: a) single NB interferer, where the interfering node is located at a fixed distance from the receiver, and b) multiple NB interferers, where the interfering nodes with the same carrier frequency are scattered according to a spatial Poisson process. Our framework is simple enough to enable a tractable analysis and provide insights that are of value in the design of practical UWB systems subject to interference.**

***Index Terms*—Ultra-wide bandwidth (UWB) communications, transmitted reference, autocorrelation receiver, energy detection, narrowband interference, Poisson point process.**

I. Introduction

ULTRA-WIDE bandwidth (UWB) signals are commonly defined as signals with a large transmission bandwidth [1]–[3]. In comparison to their narrowband (NB) counterpart, UWB systems offer a number of advantages, including accurate ranging [4]–[10], robustness to fading [11]–[13], superior obstacle penetration [14]–[16], covert operation [17], resistance to jamming and interference rejection [18], [19]. Another appealing characteristic of UWB signals is that they can be transmitted and received without any frequency conversion operation. This makes the transceiver less reliant on expensive and power-hungry oscillators. To support this low-complexity objective, a receiver cannot rely on typical digital signal processing based on sampling at least at the Nyquist rate, which for UWB signals can easily exceed several GHz.

Motivated by low-complexity implementation, transmission schemes that are suitable for non-coherent reception are considered in the IEEE 802.15.4a standard [20], [21]. There are two popular non-coherent UWB receiver structures, namely the autocorrelation receiver (AcR) and the energy detection receiver (EDR) [22]–[33]. The AcR consists of a frontend filter, a delay element and a multiplier, which are used to align and multiply the filtered received signal with its delay version prior to energy collection in the integrator. On the other hand, the EDR collects the energy of the received signal over a given time and frequency window using a frontend filter, a square-law device, and an energy integrator.

The performance of AcR and EDR for UWB systems was investigated in the litterature. The bit error probability (BEP) expressions for AcRs conditioned on an UWB channel realization using the Gaussian approximation are provided in [22]–[24]. In [25], the BEP of AcR is derived using the approach of [26] by representing the output of the AcR as a Hermitian quadratic form in complex normal variates. This approach implicitly assumes that the fading distribution of the multipath gains are Rayleigh distributed. Without any assumption on the fading distribution, the closed-form BEP expression of AcR is derived in [27]. A delay-hopped transmitted reference (TR) system is demonstrated experimentally in [28]. The effect of the NB interference on AcR was investigated and several mitigation techniques were discussed in [29], [30]. The BEP expressions of AcRs in multipath fading channel with a single NB interferer are derived in [31]. In [32], the conditional BEP expression for EDR is derived using a Gaussian approximation and the BEP performance is obtained by quasi-analytical/simulation approach. The robustness of EDR to NB interference and the effect of the NB interference bandwidth are discussed in [33]. However, an unified analytical comparison between the AcR and the EDR in the presence of multipath fading and NB interference is

Manuscript received February 13, 2008; revised October 28, 2008 and December 21, 2009; accepted January 30, 2010. The associate editor coordinating the review of this paper and approving it for publication was T. Davidson.

This research was supported, in part, by the Centre for Wireless Communication of Oulu University, Finland, the MIT Institute for Soldier Nanotechnologies, the Office of Naval Research Presidential Early Career Award for Scientists and Engineers (PECASE) N00014-09-1-0435, and the National Science Foundation under grant ECCS-0901034. This paper was presented in part at the IEEE International Conference on Ultra-Wideband, Singapore, September 2007 and the IEEE International Conference on Ultra-Wideband, Hannover, Germany, September 2008.

A. Rabbachin is with the Institute for the Protection and Security of the Citizen of the Joint Research Center, European Commission, 21027 Ispra, Italy (e-mail: alberto.rabbachin@jrc.ec.europa.eu).

T. Q. S. Quek is with the Institute for Infocomm Research, A*STAR, 1 Fusionopolis Way, #21-01 Connexis, Singapore 138632 (e-mail: qsquek@ieee.org).

I. Oppermann is with the CSIRO ICT Centre, PO Box 76, Epping, NSW 1710, Australia (e-mail: ian.oppermann@csiro.au).

P. C. Pinto and M. Z. Win are with the Laboratory for Information & Decision Systems (LIDS), Massachusetts Institute of Technology, 77 Massachusetts Avenue, Cambridge, MA 02139, USA (e-mail: {ppinto, moewin}@mit.edu).

Digital Object Identifier 10.1109/TWC.2010.091510.080203

1536-1276/10$25.00 © 2010 IEEE

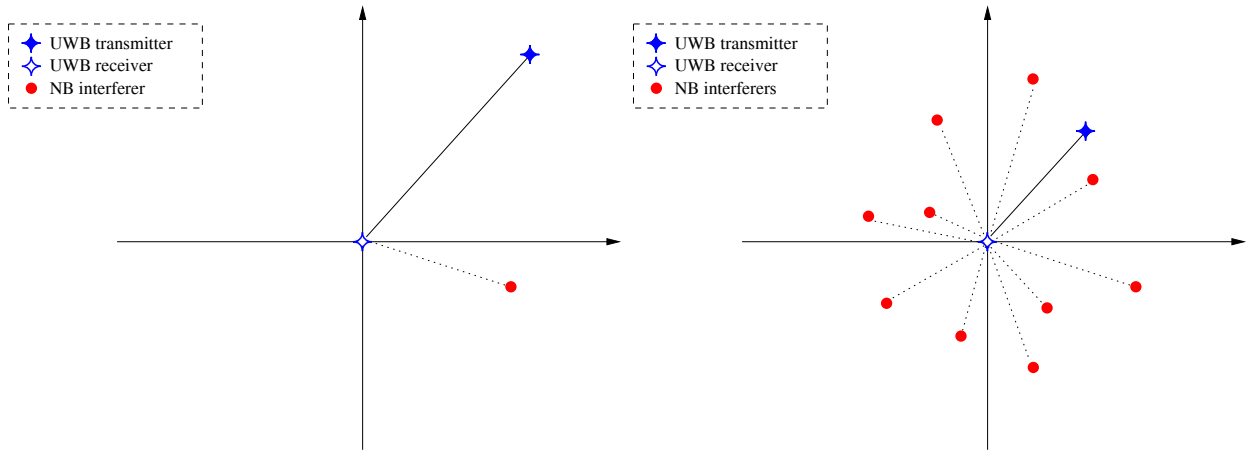

(a) Single interferer (b) Multiple interferers

Fig. 1. Interference scenarios.

still missing in the literature. Furthermore, due to their large transmission bandwidth, UWB systems need to coexist and contend with many narrowband communication systems. As a result, it is also important to analyze the performance of such receiver structures in the presence of multiple NB systems for successful deployment of UWB systems.

In this paper, we propose a framework for the performance evaluation of non-coherent UWB systems in the presence of multiple NB interferers. In particular, we compare the performance of two UWB non-coherent systems: an AcR for TR signaling with binary pulse amplitude modulation (AcR-TR-BPAM), and an EDR for binary pulse position modulation (EDR-BPPM). We consider that these systems are subject to multipath fading, and analyze two different interference scenarios: a) single NB interferer, where the interfering node is located at a fixed distance from the receiver, and b) multiple NB interferers, where the interfering nodes with the same carrier frequency are scattered according to a spatial Poisson process [34]. Our framework can be easily extended to the case where multiple NB interferers are operating at different carrier frequencies. In the absence of NB interference, we show that the two non-coherent receivers perform equally under certain conditions on pulse energy and signaling structure. In the presence of NB interference, we show that the EDR-based system is more robust than the AcR-based system. Our framework is simple enough to enable a tractable analysis and provide insights that can be of value in the design of practical UWB systems subject to interference.

The paper is organized as follows. Section II presents the system model. Section III derives expressions for the BEP in the absence of interference. Section IV and V consider the BEP with single and multiple NB interferers, respectively. Section VI provides numerical results to illustrate how the effect of NB interference depends on various system parameters. Section VII concludes the paper and summarizes the main results.

II. System Model

A. Spatial Distribution of the NB Interferers

In this paper, we consider both cases of single and multiple NB interferers, as shown in Fig. 1. In the latter case, we model the spatial distribution of the multiple NB interferers according to an homogeneous Poisson point process in the two-dimensional plane [34]-[38]. The probability that k nodes lie inside region $\mathcal{R}$ depends only on the area $A_{\mathcal{R}} = |\mathcal{R}|$, and is given by [39]

$$\mathbb{P}\{k \in \mathcal{R}\} = \frac{(\lambda A_{\mathcal{R}})^k}{k!} e^{-\lambda A_{\mathcal{R}}} \tag{1}$$

where λ is the spatial density (in nodes per unit area) of interferers that are transmitting with the same carrier frequency within the bandwidth of the receiver.

B. Transmission Characteristics of the Nodes

1) NB Nodes: It was shown in [40] that the transmitted NB signal of the n-th interferer can be well approximated by a single-tone interference for the purposes of determining the error probability, i.e.,

$$s_{\mathrm{N}}^{(n)}(t) = \sqrt{2}\cos(2\pi f_{\mathrm{J}} t) \tag{2}$$

where f_{J} is the carrier frequency. We consider the NB interference to be within the band of interest of the signal.

2) UWB TR-BPAM Nodes: In this case, the transmitted signal for user k can be decomposed into a reference signal $b_{\mathrm{r}}^{(k)}(t)$ and a data modulated signal $b_{\mathrm{d}}^{(k)}(t)$ as follows:

$$s_{\mathrm{TR}}^{(k)}(t) = \sum_i b_{\mathrm{r}}^{(k)}(t - iT_{\mathrm{s}}) + d_i^{(k)} b_{\mathrm{d}}^{(k)}(t - iT_{\mathrm{s}}) \tag{3}$$

where $d_i^{(k)} \in \{-1, 1\}$ is the ith data symbol, and $T_{\mathrm{s}} = N_{\mathrm{s}} T_{\mathrm{f}}^{\mathrm{TR}}$ is the symbol duration with N_{s} and $T_{\mathrm{f}}^{\mathrm{TR}}$ denoting the number of pulses per symbol and the average pulse repetition period, respectively [27]. The reference and data modulated signals

can be written as

$$b_{\rm r}^{(k)}(t) = \sum_{j=0}^{\frac{N_{\rm s}}{2}-1} \sqrt{E_{\rm p}^{\rm TR}} a_j^{(k)} p(t - j2T_{\rm f}^{\rm TR} - c_j^{(k)} T_{\rm p}),$$
$$b_{\rm d}^{(k)}(t) = \sum_{j=0}^{\frac{N_{\rm s}}{2}-1} \sqrt{E_{\rm p}^{\rm TR}} a_j^{(k)} p(t - j2T_{\rm f}^{\rm TR} - c_j^{(k)} T_{\rm p} - T_{\rm r}) \tag{4}$$

where $b_{\rm d}^{(k)}(t)$ is equal to a version of $b_{\rm r}^{(k)}(t)$ delayed by $T_{\rm r}$. In TH signaling, $\{c_j^{(k)}\}$ is the pseudo-random sequence of the kth user, where $c_j^{(k)}$ is an integer in the range $0 \le c_j^{(k)} < N_{\rm h}$, and $N_{\rm h}$ is the maximum allowable integer shift. The bipolar random amplitude sequence $\{a_j^{(k)}\}$ together with the TH sequence are used to mitigate interference and to support multiple access. The essential duration of the unit energy bandpass pulse $p(t)$ is $T_{\rm p}$ and its center frequency is $f_{\rm c}$. The energy of the transmitted pulse is $E_{\rm p}^{\rm TR} = E_{\rm s}^{\rm TR}/N_{\rm s}$ where $E_{\rm s}^{\rm TR}$ is the symbol energy associated with TR signaling. Note that the transmitted energy is equally allocated among $N_{\rm s}/2$ reference pulses and $N_{\rm s}/2$ modulated pulses. The duration of the received UWB pulse is $T_{\rm g} = T_{\rm p} + T_{\rm d}$, where $T_{\rm d}$ is the maximum excess delay of the channel. We consider $T_{\rm r} \ge T_{\rm g}$ and $(N_{\rm h}-1)T_{\rm p} + T_{\rm r} + T_{\rm g} \le 2T_{\rm f}^{\rm TR}$, where $T_{\rm r}$ is the time separation between each pair of data and reference pulses to preclude intra-symbol interference (isi) and inter-symbol interference (ISI).

3) UWB BPPM Nodes: In this case, the transmitted signal for user k can be expressed as

$$s_{\rm BPPM}^{(k)}(t) = \sum_i \left[\frac{(1+d_i^{(k)})}{2} b_1^{(k)}(t - iT_{\rm s}) + \frac{(1-d_i^{(k)})}{2} b_2^{(k)}(t - iT_{\rm s}) \right] \tag{5}$$

where $d_i^{(k)} \in \{-1, 1\}$ is the ith data symbol and $T_{\rm s} = \frac{N_{\rm s}}{2} T_{\rm f}^{\rm ED}$ is the symbol duration with $N_{\rm s}$ and $T_{\rm f}^{\rm TR}$ denoting the number of pulses per symbol and the average pulse repetition period, respectively.[1] The transmitted signal for $d_i^{(k)} = +1$ and $d_i^{(k)} = -1$ can be written, respectively, as

$$b_1^{(k)}(t) = \sum_{j=0}^{\frac{N_{\rm s}}{2}-1} \sqrt{E_{\rm p}^{\rm ED}} a_j^{(k)} p(t - jT_{\rm f}^{\rm ED} - c_j^{(k)} T_{\rm p}),$$
$$b_2^{(k)}(t) = \sum_{j=0}^{\frac{N_{\rm s}}{2}-1} \sqrt{E_{\rm p}^{\rm ED}} a_j^{(k)} p(t - jT_{\rm f}^{\rm ED} - c_j^{(k)} T_{\rm p} - \Delta) \tag{6}$$

where the parameter Δ is the time shift between two different data symbols and the rest of the terms in (6) are defined similarly as in (4). For BPPM with non-coherent receivers, the bipolar random amplitude sequence $\{a_j^{(k)}\}$ can only serve the purpose of spectrum smoothing. The energy of the transmitted pulse is then $E_{\rm p}^{\rm ED} = \frac{2E_{\rm s}^{\rm ED}}{N_{\rm s}}$, where $E_{\rm s}^{\rm ED}$ is the symbol energy associated with BPPM. Note that the position modulation is used and the transmitted energy is allocated among $N_{\rm s}/2$ modulated pulses. To preclude isi and ISI, we assume $\Delta \ge T_{\rm g}$ and $(N_{\rm h}-1)T_{\rm p} + \Delta + T_{\rm g} \le T_{\rm f}^{\rm ED}$.

[1]Note that we set $T_{\rm f}^{\rm TR} = \frac{T_{\rm f}^{\rm ED}}{2}$ so that the symbol durations of the two signaling schemes are the same.

C. Wireless Propagation Characteristics

1) NB Propagation: We consider that the impulse response of the NB channel between the n-th interferer and the UWB receiver is given by

$$h_{\rm N}^{(n)}(t) = \frac{1}{R_n^{\nu}} \alpha_n e^{\sigma_{\rm I} G_n} \delta(t - \tau_n). \tag{7}$$

We consider α_n to be Rayleigh distributed with $\mathbb{E}\{|\alpha_n|^2\} = 1$, which is an appropriate model when the signals are NB [41], [42]. The term τ_n accounts for the asynchronism between the interferers. The shadowing term $e^{\sigma_{\rm I} G_n}$ follows a log-normal distribution with shadowing parameter $\sigma_{\rm I}$ and $G_n \backsim \mathcal{N}(0,1)$.[2] According to the far-field assumption, the signal power decays as $1/R_n^{2\nu}$, where ν is the amplitude loss exponent and R_n is the distance between the nth interferer and the UWB receiver.[3]

2) UWB Propagation: We consider that the impulse response of the UWB channel is given by [12], [14]

$$\widetilde{h}_{\rm U}(t) = \frac{1}{R_{\rm U}^{\nu}} e^{\sigma_{\rm U} G_{\rm U}} h_{\rm U}(t) \tag{8}$$

where

$$h_{\rm U}(t) = \sum_{l=1}^{L} h_l \delta(t - \tau_l) \tag{9}$$

with h_l and τ_l representing the attenuation and the delay of the lth path component, respectively. We consider a resolvable dense multipath channel, i.e., $|\tau_l - \tau_j| \ge T_{\rm p}, \forall l \ne j$, where $\tau_l = \tau_1 + (l-1)T_{\rm p}$, and $\{h_l\}_{l=1}^{L}$ are statistically independent random variables (r.v.'s). We can express $h_l = |h_l| \exp(j\phi_l)$, where $\phi_l = 0$ or π with equal probability. We consider that the terms $\frac{1}{R_{\rm U}^{\nu}}$ and $e^{\sigma_{\rm U} G_{\rm U}}$ representing the path-loss and the shadowing in (8) are quasi-static, and therefore can be treated as constant gains introduced by the UWB channel. Thus, for simplicity, we will use $h_{\rm U}(t)$ instead of $\widetilde{h}_{\rm U}(t)$ to represent the channel impulse response between the UWB transmitter and the UWB receiver for the rest of the paper.

III. BEP in the Absence of Interference

A. AcR-TR-BPAM

As shown in Fig. 2, the AcR first passes the received signal through an ideal bandpass zonal filter (BPZF) with center frequency $f_{\rm c}$ to eliminate out-of-band noise [27], [31]. If the bandwidth W of the BPZF is large enough, then the signal spectrum will pass through the filter undistorted. In the rest of the paper, we focus on a single UWB user system and we will suppress the index k for notational simplicity. In the absence of interference, the received signal can be expressed as $r_{\rm TR}(t) = h_{\rm U}(t) * s_{\rm TR}(t) + n(t)$, where $n(t)$ is zero-mean,

[2]We use $\mathcal{N}(0, \sigma^2)$ to denote a Gaussian distribution with zero-mean and variance σ^2.

[3]Note that the amplitude loss exponent is ν, while the corresponding power loss exponent is 2ν. The parameter ν can approximately range from 0.8 (e.g. hallways inside buildings) to 4 (e.g. dense urban environment), where $\nu = 1$ corresponds to free space propagation [43].

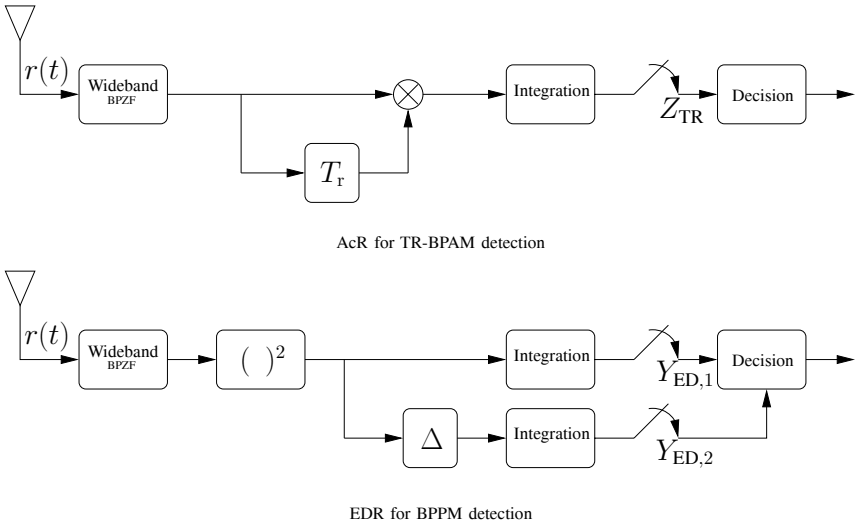

Fig. 2. UWB non-coherent receiver structures.

white Gaussian noise with two-sided power spectral density $N_0/2$. Using (3) and (9), we can write the output of the BPZF as[4]

$$\widetilde{r}_{\mathrm{TR}}(t) = \sum_i \sum_{l=1}^{L} [h_l b_{\mathrm{r}}(t - iT_{\mathrm{s}} - \tau_l) + h_l d_i b_{\mathrm{d}}(t - iT_{\mathrm{s}} - \tau_l)] + \widetilde{n}(t) \tag{10}$$

where $\widetilde{n}(t)$ represents the noise process after the BPZF, and the output of the AcR can be written as

$$Z_{\mathrm{TR}} = \sum_{j=0}^{\frac{N_{\mathrm{s}}}{2}-1} \int_{j2T_{\mathrm{f}}^{\mathrm{TR}}+T_{\mathrm{r}}+c_jT_{\mathrm{p}}}^{j2T_{\mathrm{f}}^{\mathrm{TR}}+T_{\mathrm{r}}+c_jT_{\mathrm{p}}+T} \widetilde{r}_{\mathrm{TR}}(t)\, \widetilde{r}_{\mathrm{TR}}(t - T_{\mathrm{r}}) dt \tag{11}$$

where the integration interval T determines the number of multipath components (or equivalently, the amount of energy) as well as the amount of noise captured by the receiver.[5]

It can be shown that Z_{TR} in (11) can be equivalently written as [27], [31]

$$\begin{aligned} Z_{\mathrm{TR}} = & \sum_{j=0}^{\frac{N_{\mathrm{s}}}{2}-1} \int_0^T \Big[\breve{b}_{\mathrm{r}}(t + j2T_{\mathrm{f}}^{\mathrm{TR}} + c_jT_{\mathrm{p}}) + \widetilde{n}(t + j2T_{\mathrm{f}}^{\mathrm{TR}} + c_jT_{\mathrm{p}})\Big] \\ & \times \Big[d_0 \breve{b}_{\mathrm{d}}(t + j2T_{\mathrm{f}}^{\mathrm{TR}} + c_jT_{\mathrm{p}} + T_{\mathrm{r}}) \\ & + \widetilde{n}(t + j2T_{\mathrm{f}}^{\mathrm{TR}} + c_jT_{\mathrm{p}} + T_{\mathrm{r}})\Big] dt \end{aligned} \tag{12}$$

where $\breve{b}_{\mathrm{r}}(t) \triangleq (b_{\mathrm{r}} * h_{\mathrm{U}} * h_{\mathrm{ZF}})(t)$, $\breve{b}_{\mathrm{d}}(t) \triangleq (b_{\mathrm{d}} * h_{\mathrm{U}} * h_{\mathrm{ZF}})(t)$, and $h_{\mathrm{ZF}}(t)$ is the impulse response of the BPZF. Note that if the symbol interval is less than the coherence time, all pairs of pulses will experience the same channel; hence $\breve{b}_{\mathrm{r}}(t+j2T_{\mathrm{f}}^{\mathrm{TR}}+c_jT_{\mathrm{p}}) = \breve{b}_{\mathrm{d}}(t+j2T_{\mathrm{f}}^{\mathrm{TR}}+c_jT_{\mathrm{p}}+T_{\mathrm{r}})$ for all $t \in (0, T)$ and j. In this case, we can simplify the expression in (12) as follows:

$$\begin{aligned} Z_{\mathrm{TR}} &= \sum_{j=0}^{\frac{N_{\mathrm{s}}}{2}-1} \int_0^T \Big[w_j(t) + \eta_{1,j}(t)\Big]\Big[d_0 w_j(t) + \eta_{2,j}(t)\Big] dt \\ &= \sum_{j=0}^{\frac{N_{\mathrm{s}}}{2}-1} U_j \end{aligned} \tag{13}$$

where we have used

$$w_j(t) \triangleq \breve{b}_{\mathrm{r}}(t + j2T_{\mathrm{f}}^{\mathrm{TR}} + c_jT_{\mathrm{p}}) = \sqrt{E_{\mathrm{p}}^{\mathrm{TR}}} a_j \sum_{l=1}^{L} h_l p(t - \tau_l),$$
$$\eta_{1,j}(t) \triangleq \widetilde{n}(t + j2T_{\mathrm{f}}^{\mathrm{TR}} + c_jT_{\mathrm{p}}),$$
$$\eta_{2,j}(t) \triangleq \widetilde{n}(t + j2T_{\mathrm{f}}^{\mathrm{TR}} + c_jT_{\mathrm{p}} + T_{\mathrm{r}})$$

all defined over the interval $[0, T]$. Note that because the noise samples are taken at least T_{g} apart, they are essentially independent, regardless of c_j.[6] We further observe that U_j is simply the integrator output corresponding to the jth received modulated monocycle. Following the sampling expansion approach in [27], [31], we can represent U_j as

$$\begin{aligned} U_j = \frac{1}{2W} \sum_{m=1}^{2WT} & \big(d_0 w_{j,m}^2 + w_{j,m}\eta_{2,j,m} \\ & + d_0 w_{j,m}\eta_{1,j,m} + \eta_{1,j,m}\eta_{2,j,m}\big) \end{aligned} \tag{14}$$

where $w_{j,m}$, $\eta_{1,j,m}$, and $\eta_{2,j,m}$ for odd m (even m) are the real (imaginary) parts of the samples of equivalent low-pass version of $w_j(t)$, $\eta_{1,j}(t)$, and $\eta_{2,j}(t)$, respectively, sampled at the Nyquist rate W over the interval $[0, T]$.[7] Conditioned on d_0 and $a_j = +1$, we can express (14) in the form of a

[4]Note that we assume perfect symbol synchronization at the receiver.

[5]Note that the optimal integration interval depends on the shape of the power dispersion profile and signal-to-noise ratio (SNR) [22], [27].

[6]As a result, no assumption on c_j is required since the above analysis is independent of $\{c_j\}$.

[7]Note that the noise samples taken with $1/W$ interval are statistically independent since the autocorrelation function of the Gaussian random process $\widetilde{n}(t)$ is $R_{\widetilde{n}(t)}(\tau) = W\mathrm{sinc}(W\tau)\cos(2\pi f_c\tau)$.

$$Y_{\mathrm{TR},1} \triangleq \frac{1}{2\sigma_{\mathrm{TR}}^2}\sum_{j=0}^{\frac{N_\mathrm{s}}{2}-1}\sum_{m=1}^{2WT}\left(\frac{1}{\sqrt{2W}}w_{j,m}+\beta_{1,j,m}\right)^2, \quad Y_{\mathrm{TR},2} \triangleq \frac{1}{2\sigma_{\mathrm{TR}}^2}\sum_{j=0}^{\frac{N_\mathrm{s}}{2}-1}\sum_{m=1}^{2WT}\beta_{2,j,m}^2,$$
$$Y_{\mathrm{TR},3} \triangleq \frac{1}{2\sigma_{\mathrm{TR}}^2}\sum_{j=0}^{\frac{N_\mathrm{s}}{2}-1}\sum_{m=1}^{2WT}\left(\frac{1}{\sqrt{2W}}w_{j,m}-\beta_{2,j,m}\right)^2, \quad Y_{\mathrm{TR},4} \triangleq \frac{1}{2\sigma_{\mathrm{TR}}^2}\sum_{j=0}^{\frac{N_\mathrm{s}}{2}-1}\sum_{m=1}^{2WT}\beta_{1,j,m}^2. \tag{17}$$

summation of squares:

$$U_{j|d_0=+1} = \sum_{m=1}^{2WT}\left[\left(\frac{1}{\sqrt{2W}}w_{j,m}+\beta_{1,j,m}\right)^2-\beta_{2,j,m}^2\right], \tag{15}$$
$$U_{j|d_0=-1} = \sum_{m=1}^{2WT}\left[-\left(\frac{1}{\sqrt{2W}}w_{j,m}-\beta_{2,j,m}\right)^2+\beta_{1,j,m}^2\right] \tag{16}$$

where

$$\beta_{1,j,m} \triangleq \frac{1}{2\sqrt{2W}}(\eta_{2,j,m}+\eta_{1,j,m}),$$
$$\beta_{2,j,m} \triangleq \frac{1}{2\sqrt{2W}}(\eta_{2,j,m}-\eta_{1,j,m})$$

are statistically independent Gaussian r.v.'s with variance $\sigma_{\mathrm{TR}}^2 = \frac{N_0}{4}$. For notational simplicity, we define the normalized r.v.'s $Y_{\mathrm{TR},1}$, $Y_{\mathrm{TR},2}$, $Y_{\mathrm{TR},3}$, and $Y_{\mathrm{TR},4}$ as shown in (17) at the top of this page.[8] Conditioned on $\{h_l\}$, $Y_{\mathrm{TR},1}$ and $Y_{\mathrm{TR},3}$ are non-central chi-squared r.v.'s, whereas $Y_{\mathrm{TR},2}$ and $Y_{\mathrm{TR},4}$ are central chi-squared r.v.'s, all having $q_{\mathrm{TR}} = N_\mathrm{s}WT$ degrees of freedom. Both $Y_{\mathrm{TR},1}$ and $Y_{\mathrm{TR},3}$ have the same non-centrality parameter given by

$$\mu_{\mathrm{TR}} = \frac{1}{2\sigma_{\mathrm{TR}}^2}\sum_{j=0}^{\frac{N_\mathrm{s}}{2}-1}\int_0^T w_j^2(t)dt = \frac{E_\mathrm{s}^{\mathrm{TR}}}{N_0}\sum_{l=1}^{L_{\mathrm{CAP}}}h_l^2 \tag{18}$$

where $L_{\mathrm{CAP}} \triangleq \lceil \min\{WT, WT_\mathrm{g}\}\rceil$ denotes the actual number of multipath components captured by the AcR.

The characteristic function (CF) of the difference between two non-central chi-squared r.v.'s (X_1 and X_2) with same degrees of freedom q is given by [44]

$$\psi(jv) = \left(\frac{1}{1+v^2}\right)^q \exp\left(\frac{-jv\mu_{X_1}}{1+jv}+\frac{jv\mu_{X_2}}{1-jv}\right) \tag{19}$$

where μ_{X_1} and μ_{X_2} are the non-centrality parameters of X_1 and X_2, respectively. Using the inversion theorem [45], we can derive the probability that $X_1 - X_2 < 0$ as

$$\mathbb{P}\{X_1-X_2<0\} = \frac{1}{2}+\frac{1}{\pi}\int_0^\infty\left(\frac{1}{1+v^2}\right)^q \times \mathfrak{Re}\left\{\frac{\exp\left(\frac{-jv\mu_{X_1}}{1+jv}+\frac{jv\mu_{X_2}}{1-jv}\right)}{jv}\right\}dv. \tag{20}$$

Letting $q = q_{\mathrm{TR}}$, $X_1 = Y_{\mathrm{TR},1}$, $X_2 = Y_{\mathrm{TR},2}$, $\mu_{X_1} = \mu_{\mathrm{TR}}$, and $\mu_{X_2} = 0$ in (20), and by further averaging with respect to μ_{TR}, the BEP of the AcR for detecting TR signaling with BPAM is given by

$$\begin{aligned}P_{\mathrm{e,TR}} &= \mathbb{E}_{\mu_{\mathrm{TR}}}\{\mathbb{P}\{Y_{\mathrm{TR},1}<Y_{\mathrm{TR},2}|d_0=+1,\mu_{\mathrm{TR}}\}\}\\ &= \frac{1}{2}+\frac{1}{\pi}\int_0^\infty\left(\frac{1}{1+v^2}\right)^{q_{\mathrm{TR}}}\mathfrak{Re}\left\{\frac{\psi_{\mu_{Y_{\mathrm{TR},1}}}\left(\frac{-jv}{1+jv}\right)}{jv}\right\}dv\\ &\triangleq P_\mathrm{e}(\psi_{\mu_{\mathrm{TR}}}(jv), q_{\mathrm{TR}})\end{aligned} \tag{21}$$

where $\psi_{\mu_{\mathrm{TR}}}(jv) \triangleq \mathbb{E}\{\exp(jv\mu_{\mathrm{TR}})\}$ is the CF of μ_{TR}. Note that (21) gives an alternative BEP expression to the one derived in [27].

B. EDR-BPPM

In the absence of interference, the received signal can be expressed as $r_{\mathrm{BPPM}}(t) = h_\mathrm{U}(t) * s_{\mathrm{BPPM}}(t) + n(t)$. Similarly to AcR, the EDR in Fig. 2 also first passes the received signal through an BPZF. In the absence of interference, the output of the BPZF can be written as

$$\begin{aligned}\widetilde{r}_{\mathrm{BPPM}}(t) = \sum_i\sum_{l=1}^{L}h_l\,[&(1-d_i)b_1(t-iT_\mathrm{s}-\tau_l)\\ &+ d_i\,b_2(t-iT_\mathrm{s}-\tau_l)] + \widetilde{n}(t)\end{aligned} \tag{22}$$

where $\widetilde{n}(t)$ represent the noise process after the BPZF. The decision variables for the EDR depends on the difference in energy of the received signals over the two observation variables. This can be written as

$$Z_{\mathrm{ED}} = \underbrace{\sum_{j=0}^{\frac{N_\mathrm{s}}{2}-1}\int_{jT_\mathrm{f}^{\mathrm{ED}}+c_jT_\mathrm{p}}^{jT_\mathrm{f}^{\mathrm{ED}}+c_jT_\mathrm{p}+T}\left(\widetilde{r}_{\mathrm{BPPM}}(t)\right)^2dt}_{\triangleq Z_{\mathrm{ED},1}} - \underbrace{\sum_{j=0}^{\frac{N_\mathrm{s}}{2}-1}\int_{jT_\mathrm{f}^{\mathrm{ED}}+c_jT_\mathrm{p}+\Delta}^{jT_\mathrm{f}^{\mathrm{ED}}+c_jT_\mathrm{p}+T+\Delta}\left(\widetilde{r}_{\mathrm{BPPM}}(t)\right)^2dt}_{\triangleq Z_{\mathrm{ED},2}} \tag{23}$$

where T is the integration interval.

The observed variables in (23) corresponding to the energy of the received signals over the two observation intervals can be written as

$$Z_{\mathrm{ED},1} = \sum_{j=0}^{\frac{N_\mathrm{s}}{2}-1}\int_0^T\left[w_{1,j}(t)+\eta_{1,j}(t)\right]^2dt,$$
$$Z_{\mathrm{ED},2} = \sum_{j=0}^{\frac{N_\mathrm{s}}{2}-1}\int_0^T\left[w_{2,j}(t)+\eta_{2,j}(t)\right]^2dt \tag{24}$$

[8] Due to the statistical symmetry of U_j with respect to d_0, we simply need to calculate the BEP conditioned on $d_0 = +1$.

where

$$w_{1,j}(t) \triangleq \frac{(1+d_0)}{2}\breve{b}_1(t+jT_{\rm f}^{\rm ED}+c_jT_{\rm p}),$$
$$w_{2,j}(t) \triangleq \frac{(1-d_0)}{2}\breve{b}_2(t+jT_{\rm f}^{\rm ED}+c_jT_{\rm p}+\Delta),$$
$$\eta_{1,j}(t) \triangleq \widetilde{n}(t+jT_{\rm f}^{\rm ED}+c_jT_{\rm p}),$$
$$\eta_{2,j}(t) \triangleq \widetilde{n}(t+jT_{\rm f}^{\rm ED}+c_jT_{\rm p}+\Delta).$$

Note that $\breve{b}_1(t) \triangleq (b_1 * h_{\rm U} * h_{\rm ZF})(t)$ and $\breve{b}_2(t) \triangleq (b_2 * h_{\rm U} * h_{\rm ZF})(t)$. For analytical convenience, we normalized the observed variables in (24). Using the sampling expansion, the normalized observed variables, $Z_{\rm ED,1}$ and $Z_{\rm ED,2}$ in the case of $d_0=+1$ become[9]

$$Y_{\rm ED,1} \triangleq \frac{1}{2\sigma_{\rm ED}^2}\sum_{j=0}^{\frac{N_{\rm s}}{2}-1}\sum_{m=1}^{2WT}\frac{(w_{1,j,m}+\eta_{1,j,m})^2}{2W},$$
$$Y_{\rm ED,2} \triangleq \frac{1}{2\sigma_{\rm ED}^2}\sum_{j=0}^{\frac{N_{\rm s}}{2}-1}\sum_{m=1}^{2WT}\frac{\eta_{2,j,m}^2}{2W} \quad (25)$$

where $w_{1,j,m}$, $\eta_{1,j,m}$, $w_{2,j,m}$, and $\eta_{2,j,m}$, for odd m (even m) are the real (imaginary) parts of the samples of the equivalent low-pass version of $w_{1,j}(t)$, $\eta_{1,j}(t)$, $w_{2,j}(t)$, and $\eta_{2,j}(t)$ respectively, sampled at the Nyquist rate W over the interval $[0,T]$. The noise samples $\frac{\eta_{1,j,m}}{\sqrt{2W}}$ and $\frac{\eta_{2,j,m}}{\sqrt{2W}}$ in (25) are statistically independent with equal variance $\sigma_{\rm ED}^2=N_0/2$. Conditioned on $\{h_l\}$, the observed variables $Y_{\rm ED,1}$ and $Y_{\rm ED,2}$ are non-central and central chi-square r.v.'s with $q_{\rm ED}=N_{\rm s}WT$ degrees of freedom, respectively. The non-centrality parameter of $Y_{\rm ED,1}$ can be written as

$$\mu_{\rm ED}=\frac{1}{2\sigma_{\rm ED}^2}\sum_{j=0}^{\frac{N_{\rm s}}{2}-1}\int_0^T w_{1,j}^2(t)dt=\frac{E_{\rm s}^{\rm ED}}{N_0}\sum_{l=1}^{L_{\rm CAP}}h_l^2. \quad (26)$$

Note that, when conditioned on the channel, the r.v.'s $Y_{\rm ED,1}$ and $Y_{\rm ED,2}$ have the same distribution as $Y_{\rm TR,1}$ and $Y_{\rm TR,2}$ in (17). Therefore, the BEP of the EDR for detecting BPPM can be expressed as

$$P_{\rm e,ED}=P_{\rm e}(\psi_{\mu_{\rm ED}}(\jmath v),q_{\rm ED}) \quad (27)$$

where $\psi_{\mu_{\rm ED}}(\jmath v) \triangleq \mathbb{E}\{\exp(\jmath v\mu_{\rm ED})\}$ is the CF of $\mu_{\rm ED}$. Comparing (21) and (27), we observe that these two systems achieve the same BEP performance as long as they have equal non-centrality parameters (see (18) and (26)).

IV. BEP with a Single Interferer

The received NB interference signal can be written, using (2) and (7), as $\xi(t)=s_{\rm N}(t)*h_{\rm N}(t)$. At the output of the BPZF the NB interference signal can be written as[10]

$$\xi(t)=\sqrt{2J_0}\alpha_{\rm J}\cos(2\pi f_{\rm J}t+\theta) \quad (28)$$

where J_0 is the average received power of the interference and $f_{\rm J}$ is the carrier frequency. The parameters $\alpha_{\rm J}$ and θ represent the amplitude and the phase, respectively, of the fading associated with the NB interference.

[9]Due to the statistical symmetry of $Z_{\rm ED}$ with respect to d_0, we simply need to consider only the BEP conditioned on $d_0=+1$.

[10]We consider a quasi-static fading channel with no shadowing. Moreover, we assume that the NB interfering signal does not saturate the amplification chain of the UWB receiver.

A. AcR-TR-BPAM

Using the sampling expansion approach in [31], it can be shown that in this case (17) still holds with

$$\beta_{1,j,m} \triangleq \frac{1}{2\sqrt{2W}}(\eta_{2,j,m}+\xi_{2,j,m}+\eta_{1,j,m}+\xi_{1,j,m}),$$
$$\beta_{2,j,m} \triangleq \frac{1}{2\sqrt{2W}}(\eta_{2,j,m}+\xi_{2,j,m}-\eta_{1,j,m}-\xi_{1,j,m}).$$

The terms $\xi_{1,j,m}$ and $\xi_{2,j,m}$, for odd m (even m) are the real (imaginary) parts of the samples of the equivalent low-pass version of

$$\xi_{1,j}(t) \triangleq \sqrt{2J_0}\alpha_{\rm J}\cos[2\pi(f_{\rm J}t+j2T_{\rm f}^{\rm TR}+c_jT_{\rm p})+\theta],$$
$$\xi_{2,j}(t) \triangleq \sqrt{2J_0}\alpha_{\rm J}\cos[2\pi(f_{\rm J}t+j2T_{\rm f}^{\rm TR}+c_jT_{\rm p}+T_{\rm r})+\theta]$$

respectively, sampled at the Nyquist rate W over the interval $[0,T]$. Furthermore, by conditioning on θ, $\{c_j\}$, $\{a_j\}$, $\{h_l\}$, and $\alpha_{\rm J}$, the conditional variance $\sigma_{\rm TR}^2$ of $\beta_{1,j,m}$ and $\beta_{2,j,m}$ is simply $\frac{N_0}{4}$, and the non-centrality parameters of $Y_{\rm TR,1}$ and $Y_{\rm TR,2}$ for $d_0=+1$ are, respectively, given by (29) and (30) shown at the top of next page, where $|\widehat{P}(f_{\rm J})|$ is the magnitude of the frequency response of $p(t)$ at frequency $f_{\rm J}$. The composite random phase is given by $\varphi \triangleq \arg\{\widehat{P}(f_{\rm J})\}+\theta$, where $\arg\{\widehat{P}(f_{\rm J})\}$ is the angle of the frequency response of $p(t)$ at frequency $f_{\rm J}$, and φ is uniformly distributed over $[0,2\pi)$. The analysis for the non-centrality parameters of $Y_{\rm TR,3}$ and $Y_{\rm TR,4}$ for $d_0=-1$ can be carried out similarly. Using (20), (29) and (30), we invoke the approximate analytical method developed in [31] to obtain the approximate BEP conditioned on $d_0=\pm1$ as follows:[11]

$$P_{\rm e,TR|d_0=\pm1}^{\rm (NBI)} \simeq \frac{1}{2}+\frac{1}{\pi}\int_0^\infty\left(\frac{1}{1+v^2}\right)^{q_{\rm TR}} \times \Re\mathfrak{e}\left\{\frac{\psi_{\mu_{\rm TR}}\left(\frac{-\jmath v}{1+\jmath v}\right)\psi_{\rm J}\left(g_{{\rm TR},d_0=\pm1}(\jmath v)\cdot J_0\right)}{\jmath v}\right\}dv \quad (31)$$

where $\psi_{\rm J}(\jmath v)$ is the CF of $\alpha_{\rm J}^2$ and

$$g_{{\rm TR}|d_0=\pm1}(\jmath v) \triangleq \frac{-\jmath v}{1+\jmath v}\frac{N_{\rm s}T}{2N_0}\Big[1\pm\cos(2\pi f_{\rm J}T_{\rm r})\Big] + \frac{\jmath v}{1-\jmath v}\frac{N_{\rm s}T}{2N_0}\Big[1\mp\cos(2\pi f_{\rm J}T_{\rm r})\Big]. \quad (32)$$

As a result, it follows that the BEP of the AcR for detecting TR signaling with BPAM in the presence of a single NB interferer is given by

$$P_{\rm e,TR}^{\rm (NBI)}=\frac{1}{2}\left(P_{\rm e,TR,d_0=+1}^{\rm (NBI)}+P_{\rm e,TR,d_0=-1}^{\rm (NBI)}\right). \quad (33)$$

B. EDR-BPPM

Similar to the steps in Section IV-A, we incorporate the NB interference given in (28) into (25) to obtain

$$Y_{\rm ED,1} = \frac{1}{2\sigma_{\rm ED}^2}\sum_{j=0}^{\frac{N_{\rm s}}{2}-1}\sum_{m=1}^{2WT}\frac{(w_{1,j,m}+\xi_{1,j,m}+\eta_{1,j,m})^2}{2W},$$
$$Y_{\rm ED,2} = \frac{1}{2\sigma_{\rm ED}^2}\sum_{j=0}^{\frac{N_{\rm s}}{2}-1}\sum_{m=1}^{2WT}\frac{(\xi_{2,j,m}+\eta_{2,j,m})^2}{2W} \quad (34)$$

[11]Under the approximate analytical method, the last term $\mu_{\rm C,TR}^{\rm (NBI)}$ in (29) is considered to be negligible compared to the first two terms.

$$\mu_{Y_{\mathrm{TR},1}}^{(\mathrm{NBI})} \triangleq \frac{1}{2\sigma_{\mathrm{TR}}^2}\sum_{j=0}^{\frac{N_\mathrm{s}}{2}-1}\int_0^T\left[w_j(t)+\frac{\xi_{1,j}(t)+\xi_{2,j}(t)}{2}\right]^2 dt$$
$$\approx \underbrace{\frac{E_\mathrm{s}^{\mathrm{TR}}}{N_0}\sum_{l=1}^{L_{\mathrm{CAP}}}h_l^2}_{\triangleq\mu_{\mathrm{A,TR}}} + \underbrace{\frac{\alpha_\mathrm{J}^2 N_\mathrm{s} J_0 T}{2N_0}[1+\cos(2\pi f_\mathrm{J} T_\mathrm{r})]}_{\triangleq\mu_{\mathrm{B,TR}}^{(\mathrm{NBI})}}$$
$$+\underbrace{\frac{4\alpha_\mathrm{J}|\widehat{P}(f_\mathrm{J})|\sqrt{2E_\mathrm{p}^{\mathrm{TR}}J_0}\cos(\pi f_\mathrm{J}T_\mathrm{r})}{N_0}\sum_{j=0}^{\frac{N_\mathrm{s}}{2}-1}a_j\sum_{l=1}^{L_{\mathrm{CAP}}}h_l\cos\left(2\pi f_\mathrm{J}\left(\tau_l+j2T_\mathrm{f}^{\mathrm{TR}}+c_jT_\mathrm{p}+T_\mathrm{r}/2\right)+\varphi\right)}_{\triangleq\mu_{\mathrm{C,TR}}^{(\mathrm{NBI})}}, \tag{29}$$

$$\mu_{Y_{\mathrm{TR},2}}^{(\mathrm{NBI})} \approx \frac{\alpha_\mathrm{J}^2 N_\mathrm{s} J_0 T}{2N_0} - \frac{\alpha_\mathrm{J}^2 N_\mathrm{s} J_0 T}{2N_0}\cos(2\pi f_\mathrm{J} T_\mathrm{r}). \tag{30}$$

$$\mu_{Y_{\mathrm{ED},1}}^{(\mathrm{NBI})} = \underbrace{\frac{1}{2\sigma_{\mathrm{ED}}^2}\sum_{j=0}^{\frac{N_\mathrm{s}}{2}-1}\int_0^T w_{1,j}^2(t)dt}_{\triangleq\mu_{\mathrm{A,ED}}} + \underbrace{\frac{1}{2\sigma_{\mathrm{ED}}^2}\sum_{j=0}^{\frac{N_\mathrm{s}}{2}-1}\int_0^T \xi_{1,j}^2(t)dt}_{\triangleq\mu_{\mathrm{B,ED}}^{(\mathrm{NBI})}} + \underbrace{\frac{1}{\sigma_{\mathrm{ED}}^2}\sum_{j=0}^{\frac{N_\mathrm{s}}{2}-1}\int_0^T w_{1,j}(t)\xi_{1,j}(t)dt}_{\triangleq\mu_{\mathrm{C,ED}}^{(\mathrm{NBI})}} \tag{35}$$

where $\xi_{1,j,m}$ and $\xi_{2,j,m}$ for odd m (even m) are the real (imaginary) parts of the samples of the equivalent low-pass version of

$$\xi_{1,j}(t) \triangleq \sqrt{2J_0}\alpha_\mathrm{J}\cos[2\pi f_\mathrm{J}(t+jT_\mathrm{f}^{\mathrm{ED}}+c_jT_\mathrm{p})+\theta],$$
$$\xi_{2,j}(t) \triangleq \sqrt{2J_0}\alpha_\mathrm{J}\cos[2\pi f_\mathrm{J}(t+jT_\mathrm{f}^{\mathrm{ED}}+c_jT_\mathrm{p}+\Delta)+\theta]$$

respectively, sampled at the Nyquist rate W over the interval $[0,T]$.

The non-centrality parameter of $Y_{\mathrm{ED},1}$ in (34) conditioned on θ, $\{c_j\}$, $\{a_j\}$, $\{h_l\}$, α_J, and $d_0=+1$ is given by (35) at the top of this page,[12] where $\mu_{\mathrm{A,ED}}$, $\mu_{\mathrm{B,ED}}^{(\mathrm{NBI})}$, and $\mu_{\mathrm{C,ED}}^{(\mathrm{NBI})}$ denote the received signal energy term, the received interference energy term, and signal-interference cross term, respectively. Specifically, we have

$$\mu_{\mathrm{A,ED}} = \frac{E_\mathrm{s}^{\mathrm{ED}}}{N_0}\sum_{l=1}^{L_{\mathrm{CAP}}}h_l^2, \tag{36}$$

$$\mu_{\mathrm{B,ED}}^{(\mathrm{NBI})} = \frac{\alpha_\mathrm{J}^2 J_0}{N_0}\sum_{j=0}^{\frac{N_\mathrm{s}}{2}-1}\left[T+\frac{\sin\left(4\pi f_\mathrm{J}(T+jT_\mathrm{f}^{\mathrm{ED}}+c_jT_\mathrm{p})+2\theta\right)}{4\pi f_\mathrm{J}} - \frac{\sin\left(4\pi f_\mathrm{J}(jT_\mathrm{f}^{\mathrm{ED}}+c_jT_\mathrm{p})+2\theta\right)}{4\pi f_\mathrm{J}}\right]$$
$$\approx \frac{\alpha_\mathrm{J}^2 N_\mathrm{s} J_0 T}{2N_0} \tag{37}$$

and $\mu_{\mathrm{C,ED}}^{(\mathrm{NBI})}$ expressed in (38) at the top of next page, where the approximation in (37) holds for UWB systems since $T \gg \frac{1}{4\pi f_\mathrm{J}}$ and $|\sin(\phi)| \le 1$.

Following the steps leading to (37), the non-centrality parameter of $Y_{\mathrm{ED},2}$ in (34) when conditioned on θ, α_J, and $d_0=+1$ is given by

$$\mu_{Y_{\mathrm{ED},2}}^{(\mathrm{NBI})} \approx \frac{\alpha_\mathrm{J}^2 N_\mathrm{s} J_0 T}{2N_0}. \tag{39}$$

By invoking the approximate analytical method, we can obtain the approximate BEP of the EDR for detecting BPPM in the presence of a single NB interferer as follows:[13]

$$P_{\mathrm{e,ED}}^{(\mathrm{NBI})} \simeq \frac{1}{2}+\frac{1}{\pi}\int_0^\infty\left(\frac{1}{1+v^2}\right)^{q_{\mathrm{ED}}} \times \mathfrak{Re}\left\{\frac{\psi_{\mu_{\mathrm{ED}}}\left(\frac{-jv}{1+jv}\right)\psi_\mathrm{J}\left(g_{\mathrm{ED}}(jv)\cdot J_0\right)}{jv}\right\}dv \tag{40}$$

where

$$g_{\mathrm{ED}}(jv) = \frac{N_\mathrm{s}T}{2N_0}\left(\frac{-jv}{1+jv}+\frac{jv}{1-jv}\right). \tag{41}$$

V. BEP with Multiple Interferers

Using (2) and (7), the aggregate interference signal can be expressed as $\zeta_n(t) = s_\mathrm{N}^{(n)}(t) * h_\mathrm{N}^{(n)}(t)$. At the output of the BPZF, the aggregate interference signal can be written as

$$\zeta(t) = \sum_{n=1}^{\infty}\zeta_n(t) \tag{42}$$

where $\zeta_n(t)$ denotes the interference signal from the nth NB interferer at the UWB receiver given by

$$\zeta_n(t) = \sqrt{2I}\frac{e^{\sigma_I G_n}}{R_n^\nu}\alpha_n\cos(2\pi f_\mathrm{J}(t-\tau_n)+\theta_n) \tag{43}$$

where I is the average power at the border of the near-field zone of each interfering transmitter antenna and τ_n accounts

[12]The statistical symmetry of Z_{ED} with respect to d_0 still holds even in the presence of interference, and hence we simply need to consider only the BEP conditioned on $d_0=+1$.

[13]As in the case for AcR, the last term $\mu_{\mathrm{C,ED}}^{(\mathrm{NBI})}$ in (35) is considered to be negligible compared to the first two terms.

$$\mu_{\mathrm{C,ED}}^{(\mathrm{NBI})} = \frac{2\alpha_{\mathrm{J}}\sqrt{2E_{\mathrm{p}}^{\mathrm{ED}}J_0}}{N_0}\sum_{j=0}^{\frac{N_{\mathrm{s}}}{2}-1} a_j \sum_{l=1}^{L_{\mathrm{CAP}}} h_l \int_{\tau_l}^{\tau_l+T_{\mathrm{p}}} p(t)\left[\cos\left(2\pi f_{\mathrm{J}}(t+\tau_l+jT_{\mathrm{f}}^{\mathrm{ED}}+c_jT_{\mathrm{p}})+\theta\right)\right]dt$$
$$= \frac{2\alpha_{\mathrm{J}}|\widehat{P}(f_{\mathrm{J}})|\sqrt{2E_{\mathrm{p}}^{\mathrm{ED}}J_0}}{N_0}\sum_{j=0}^{\frac{N_{\mathrm{s}}}{2}-1} a_j \sum_{l=1}^{L_{\mathrm{CAP}}} h_l\left[\cos\left(2\pi f_{\mathrm{J}}\left(\tau_l+jT_{\mathrm{f}}^{\mathrm{ED}}+c_jT_{\mathrm{p}}\right)+\varphi\right)\right]. \quad (38)$$

$$\mu_{Y_{\mathrm{TR},1}}^{(\mathrm{NBIs})} \approx \frac{E_{\mathrm{s}}^{\mathrm{TR}}}{N_0}\sum_{l=1}^{L_{\mathrm{CAP}}} h_l^2 + \frac{|\mathbf{A}|^2ITN_{\mathrm{s}}}{2N_0}\Big[1+\cos(2\pi f_{\mathrm{J}}T_{\mathrm{r}})\Big] + \frac{4|\widehat{P}(f_{\mathrm{J}})|\sqrt{2E_{\mathrm{p}}^{\mathrm{TR}}J_0}}{N_0}$$
$$\times \sum_{j=0}^{\frac{N_{\mathrm{s}}}{2}-1} a_j \sum_{l=1}^{L_{\mathrm{CAP}}} h_l\left[A_{\mathrm{c}}\cos\left(\pi f_{\mathrm{J}}T_{\mathrm{r}}\right)\cos\left(2\pi f_{\mathrm{J}}\left(\tau_l+j2T_{\mathrm{f}}^{\mathrm{TR}}+c_jT_{\mathrm{p}}+T_{\mathrm{r}}/2\right)+\tilde{\varphi}\right)\right.$$
$$\left. -A_{\mathrm{s}}\cos\left(\pi f_{\mathrm{J}}T_{\mathrm{r}}\right)\sin\left(2\pi f_{\mathrm{J}}\left(\tau_l+j2T_{\mathrm{f}}^{\mathrm{TR}}+c_jT_{\mathrm{p}}+T_{\mathrm{r}}/2\right)+\tilde{\varphi}\right)\right], \quad (48)$$

$$\mu_{Y_{\mathrm{TR},2}}^{(\mathrm{NBIs})} \approx \frac{|\mathbf{A}|^2ITN_{\mathrm{s}}}{2N_0}\Big[1-\cos(2\pi f_{\mathrm{J}}T_{\mathrm{r}})\Big]. \quad (49)$$

for the asynchronism between the interferers. The parameters α_n and θ_n denote the amplitude and phase, respectively, of the fading associated with the nth interferer. For notational convenience, we defined $\phi_n = 2\pi f_{\mathrm{J}}\tau_n + \theta_n$.

We can equivalently write (43) as

$$\zeta_n(t) = \sqrt{2I}\mathfrak{Re}\left\{\frac{e^{\sigma_I G_n}}{R_n^{\nu}}\mathbf{X}_n e^{\jmath 2\pi f_{\mathrm{J}}t}\right\} \quad (44)$$

where $\mathbf{X}_n = X_{n,1} + \jmath X_{n,2}$ is a circularly symmetric (CS) Gaussian r.v. with $X_{n,1} = \alpha_n\cos(\phi_n)$ and $X_{n,2} = \alpha_n\sin(\phi_n)$. The aggregate interference signal over the period T_{s} can be represented as

$$\zeta(t) = \sqrt{2I}\mathfrak{Re}\left\{\mathbf{A}e^{\jmath 2\pi f_{\mathrm{J}}t}\right\} \quad (45)$$

where $\mathbf{A} = A_{\mathrm{c}} + \jmath A_{\mathrm{s}}$ such that $A_{\mathrm{c}} \triangleq \sum_{n=1}^{\infty}\frac{e^{\sigma_I G_n}}{R_n^{\nu}}X_{n,1}$ and $A_{\mathrm{s}} \triangleq \sum_{n=1}^{\infty}\frac{e^{\sigma_I G_n}}{R_n^{\nu}}X_{n,2}$.[14] As shown in Appendix A, the complex r.v. $\mathbf{A}$ is characterized by a CS stable distribution[15]

$$\mathbf{A} \sim \mathcal{S}_{\mathrm{c}}\left(\frac{2}{\nu},\, 0,\, \pi\lambda C_{2/\nu}^{-1}e^{2\sigma_I^2/\nu^2}\mathbb{E}\left\{|X_{n,j}|^{2/\nu}\right\}\right) \quad (46)$$

with C_x defined as

$$C_x \triangleq \begin{cases}\frac{1-x}{\Gamma(2-x)\cos(\pi x/2)}, & x\neq 1,\\ \frac{2}{\pi}, & x=1.\end{cases} \quad (47)$$

Interestingly, (45) and (46) imply that the aggregate interference can be thought as a single NB interferer with complex CS stable fading.[16]

[14]We consider the fading and the mobility of the interferers to be slow enough such that $\mathbf{A}$ is constant within the period T_{s}.

[15]We use $\mathcal{S}_{\mathrm{c}}(\alpha,\beta,\gamma)$ to denote a CS stable distribution of a complex r.v. with real and imaginary parts, each distributed as $\mathcal{S}(\alpha,\beta,\gamma)$, with characteristic exponent α, skewness β (i.e. $\beta = 0$ in our case), and dispersion γ. For $\alpha \neq 1$ and $\alpha = 1$, the associated CFs are $\psi(\jmath v) = \exp\left[-\gamma|\jmath v|^{\alpha}\left(1-\jmath\beta\frac{\jmath v}{|\jmath v|}\tan(\frac{\pi\alpha}{2})\right)\right]$ and $\psi(\jmath v) = \exp\left[-\gamma|\jmath v|\left(1-\jmath\beta\frac{\jmath v}{|\jmath v|}\ln|\jmath v|\right)\right]$, respectively [46].

[16]Note that in the case of CS stable distribution the real and imaginary components are uncorrelated but not necessarily independent.

A. AcR-TR-BPAM

Following the approach in Section IV-A, we derive the non-centrality parameters of $Y_{\mathrm{TR},1}$ and $Y_{\mathrm{TR},2}$ when conditioned on $\mathbf{A}$, $\{c_j\}$, $\{a_j\}$, $\{h_l\}$, and $d_0 = +1$ as shown in (48) and (49) at the top of this page, where $\tilde{\varphi} = \arg\{\widehat{P}(f_{\mathrm{J}})\}$ and the derivation of (48) and (49) can be found in Appendix B. The analysis for the non-centrality parameters of $Y_{\mathrm{TR},3}$ and $Y_{\mathrm{TR},4}$ for $d_0 = -1$ can be carried out similarly. Using the approximate analytical method, it follows from (20), (48), and (49) that the approximate BEP of the AcR for detecting TR signaling with BPAM conditioned on $\mathbf{A}$ and $d_0 = \pm 1$ is given by

$$P_{\mathrm{e,TR}|\mathbf{A},d_0=\pm1}^{(\mathrm{NBIs})} \quad (50)$$
$$\simeq \frac{1}{2} + \frac{1}{\pi}\int_0^{\infty}\left(\frac{1}{1+v^2}\right)^{q_{\mathrm{TR}}} \times \mathfrak{Re}\left\{\frac{\psi_{\mu_{\mathrm{TR}}}\left(\frac{-\jmath v}{1+\jmath v}\right)\exp\left(g_{\mathrm{TR},d_0=\pm1}(\jmath v)\cdot I|\mathbf{A}|^2\right)}{\jmath v}\right\}dv.$$

It follows from (63) Appendix A that

$$|\mathbf{A}|^2 = 2\gamma^{\nu}VC \quad (51)$$

where C is a central chi-squared distributed r.v. with two degrees of freedom. Applying the scaling property,[17] $|\mathbf{A}|^2$ conditioned on C is stable distributed with characteristic exponent $1/\nu$, skewness 1 and dispersion $(2C)^{1/\nu}\gamma\cos\left(\frac{\pi}{2\nu}\right)$. The CF of $|\mathbf{A}|^2$ conditioned on C for $\nu > 1$ is given by

$$\psi_{|\mathbf{A}|^2|C}(\jmath v) \quad (52)$$
$$= \exp\left\{-(2C)^{1/\nu}\gamma\cos\left(\frac{\pi}{2\nu}\right)|\jmath v|^{1/\nu}\left[1-\frac{\jmath v}{|\jmath v|}\tan\left(\frac{\pi}{2\nu}\right)\right]\right\}.$$

[17]The scaling property states that if $X \sim S(\alpha,\beta,\gamma)$, then $kX \sim S(\alpha, \mathrm{sign}(k)\beta, |k|^{\alpha}\gamma)$ for any non-zero real constant k [46].

$$\mu_{Y_{\mathrm{ED},1}}^{(\mathrm{NBIs})} \approx \frac{E_{\mathrm{s}}^{\mathrm{ED}}}{N_0}\sum_{l=1}^{L_{\mathrm{CAP}}} h_l^2 + \frac{|\mathbf{A}|^2 I T N_{\mathrm{s}}}{2N_0} + \frac{2|\widehat{P}(f_{\mathrm{J}})|\sqrt{2E_{\mathrm{p}}^{\mathrm{ED}} I}}{N_0}\sum_{j=0}^{\frac{N_{\mathrm{s}}}{2}-1} a_j \sum_{l=1}^{L_{\mathrm{CAP}}} h_l \times \left[A_{\mathrm{c}}\cos\left(2\pi f_{\mathrm{J}}\left(\tau_l + jT_{\mathrm{f}}^{\mathrm{ED}} + c_j T_{\mathrm{p}}\right) + \tilde{\varphi}\right) - A_{\mathrm{s}}\sin\left(2\pi f_{\mathrm{J}}\left(\tau_l + jT_{\mathrm{f}}^{\mathrm{ED}} + c_j T_{\mathrm{p}}\right) + \tilde{\varphi}\right)\right] \tag{58}$$

$$\mu_{Y_{\mathrm{ED},2}}^{(\mathrm{NBIs})} \approx \frac{|\mathbf{A}|^2 I T N_{\mathrm{s}}}{2N_0} \tag{59}$$

The approximated BEP conditioned on C and $d_0 = \pm 1$ can be written as

$$P_{\mathrm{e,TR}|C,d_0=\pm1}^{(\mathrm{NBIs})} \simeq \frac{1}{2} + \frac{1}{\pi}\int_0^\infty \left(\frac{1}{1+v^2}\right)^{q_{\mathrm{TR}}} \times \Re\mathfrak{e}\left\{\frac{\psi_{\mu_{\mathrm{TR}}}\left(\frac{-jv}{1+jv}\right)\psi_{|\mathbf{A}|^2|C}\left(g_{\mathrm{TR},d_0=\pm1}(jv)\cdot I\right)}{jv}\right\} dv \tag{53}$$

where $g_{\mathrm{TR},d_0=\pm1}(jv)$ is defined in (32). The total approximated BEP conditioned on C can be expressed as

$$P_{\mathrm{e,TR}|C}^{(\mathrm{NBIs})} \simeq \frac{1}{2}\left(P_{\mathrm{e,TR}|C,d_0=+1}^{(\mathrm{NBIs})} + P_{\mathrm{e,TR}|C,d_0=-1}^{(\mathrm{NBIs})}\right). \tag{54}$$

Compared to (50), we only need to numerically average over C, which is computationally much more attractive. However, we can also avoid this averaging by approximating the CF of $|\mathbf{A}|^2$ over a certain range of ν. We can approximate the expectation of (52) with respect to C as follows:

$$\psi_{|\mathbf{A}|^2}(jv) \simeq \left[1 + \Omega_\nu 2^{1/\nu}\gamma\cos\left(\frac{\pi}{2\nu}\right)|jv|^{1/\nu}\left(1 - \frac{jv}{|jv|}\tan\left(\frac{\pi}{2\nu}\right)\right)\right]^{-k_\nu} \tag{55}$$

where we have used Gamma distribution to approximate the distribution of $C^{1/\nu}$. Using (50) and (55), the approximate BEP of the AcR for detecting TR signaling with BPAM in the presence of multiple NB interferers conditioned on $d_0 = \pm 1$ is given by

$$P_{\mathrm{e,TR}|d_0=\pm1}^{(\mathrm{NBIs})} \simeq \frac{1}{2} + \frac{1}{\pi}\int_0^\infty \left(\frac{1}{1+v^2}\right)^{q_{\mathrm{TR}}} \times \Re\mathfrak{e}\left\{\frac{\psi_{\mu_{\mathrm{TR}}}\left(\frac{-jv}{1+jv}\right)\psi_{|\mathbf{A}|^2}\left(g_{\mathrm{TR},d_0=\pm1}(jv)\cdot I\right)}{jv}\right\} dv. \tag{56}$$

As a result, it follows that the BEP of the AcR for detecting TR signaling with BPAM in the presence of multiple NB interferers is given by

$$P_{\mathrm{e,TR}}^{(\mathrm{NBIs})} = \frac{1}{2}\left(P_{\mathrm{e,TR},d_0=+1}^{(\mathrm{NBIs})} + P_{\mathrm{e,TR},d_0=-1}^{(\mathrm{NBIs})}\right). \tag{57}$$

B. EDR-BPPM

Following the approach in Section IV-B, we derive the non-centrality parameters of $Y_{\mathrm{ED},1}$ and $Y_{\mathrm{ED},2}$ conditioned on $\mathbf{A}$, $\{c_j\}$, $\{a_j\}$, $\{h_l\}$ and $d_0 = +1$ as given in (58)-(59) at the top of this page, whose derivation follows straightforwardly from Appendix B. Similar to Section V-A, the approximated BEP of the EDR for detecting BPPM conditioned on C in the presence of multiple NB interferers is given by

$$P_{\mathrm{e,ED}|C}^{(\mathrm{NBIs})} \simeq \frac{1}{2} + \frac{1}{\pi}\int_0^\infty \left(\frac{1}{1+v^2}\right)^{q_{\mathrm{ED}}} \times \Re\mathfrak{e}\left\{\frac{\psi_{\mu_{\mathrm{ED}}}\left(\frac{-jv}{1+jv}\right)\psi_{|\mathbf{A}|^2|C}\left(g_{\mathrm{ED}}(jv)\cdot I\right)}{jv}\right\} dv \tag{60}$$

where g_{ED} is defined in (41). Alternatively, numerical averaging can be avoided by using the approximate CF in (55), and we can obtain the BEP of the EDR for detecting the BPPM signal in the presence of multiple interference as

$$P_{\mathrm{e,ED}}^{(\mathrm{NBIs})} \simeq \frac{1}{2} + \frac{1}{\pi}\int_0^\infty \left(\frac{1}{1+v^2}\right)^{q_{\mathrm{ED}}} \times \Re\mathfrak{e}\left\{\frac{\psi_{\mu_{\mathrm{ED}}}\left(\frac{-jv}{1+jv}\right)\psi_{|\mathbf{A}|^2}\left(g_{\mathrm{ED}}(jv)\cdot I\right)}{jv}\right\} dv. \tag{61}$$

VI. Numerical results

In this section, we evaluate the performance of both AcR with TR signaling and EDR with BPPM signaling, with single and multiple NB interferers, using analytical expressions developed in Sections IV and V. Note that all BEP numerical results shown are based on the approximate analytical method. We consider a bandpass UWB system with pulse duration $T_{\mathrm{p}} = 0.5$ ns, symbol interval $T_{\mathrm{s}} = 3200$ ns, and $N_{\mathrm{s}} = 32$. For simplicity, T_{r} and Δ are set such that there is no ISI or isi in the system, i.e., $T_{\mathrm{r}} = 2T_{\mathrm{f}}^{\mathrm{TR}} - T_{\mathrm{g}} - N_{\mathrm{h}}T_{\mathrm{p}}$ and $\Delta = T_{\mathrm{f}}^{\mathrm{ED}} - T_{\mathrm{g}} - N_{\mathrm{h}}T_{\mathrm{p}}$. We consider a TH sequence of all ones ($c_j = 1$ for all j) and $N_{\mathrm{h}} = 2$. For UWB channels, we consider a dense resolvable multipath channel, where each multipath gain is Nakagami distributed with fading severity index m and average power $\mathbb{E}\{h_l^2\}$, where $\mathbb{E}\{h_l^2\} = \mathbb{E}\{h_1^2\}\exp[-\epsilon(l-1)]$, for $l = 1, \ldots, L$, are normalized such that $\sum_{l=1}^{L}\mathbb{E}\{h_l^2\} = 1$ [14]. For simplicity, the fading severity index m is assumed to be identical for all paths. The average power of the first arriving multipath component is given by $\mathbb{E}\{h_1^2\}$, and ϵ is the channel power decay constant. With this model, we parameterize the UWB channel by (L, ϵ, m) for convenience. For the NB channels, we assume that the NB interference is within the band of interest and experiences flat Rayleigh fading, i.e., the CF of α_{J} is $\psi_{\mathrm{J}}(jv) = 1/(1-jv)$. To compare AcR-TR-BPAM and EDR-BPPM systems, we let $E_{\mathrm{s}}^{\mathrm{TR}} = E_{\mathrm{s}}^{\mathrm{ED}} = E_{\mathrm{b}}$, with E_{b} denoting the energy per bit. We define the signal-to-interference ratios as $\mathsf{SIR} \triangleq E_{\mathrm{b}}/(J_0 T_{\mathrm{s}})$ and $\mathsf{SIR}_{\mathsf{T}} \triangleq E_{\mathrm{b}}/(IT_{\mathrm{s}})$ for the cases of single NB interferer and of multiple NB interferers, respectively.

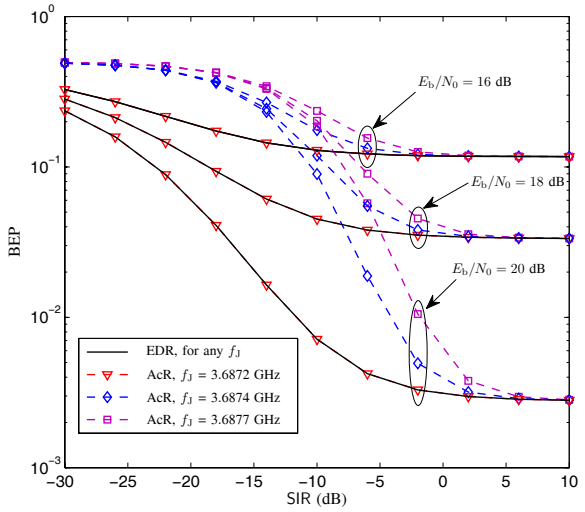

Fig. 3. BEP comparison of UWB non-coherent receiver structures in the presence of a single NB interferer. The dashed and solid lines indicate the AcR-TR-BPAM system and EDR-BPPM system, respectively. Note that AcR-TR-BPAM and EDR-BPPM for the selected T_r and $f_J = 3.6872$ GHz give identical results.

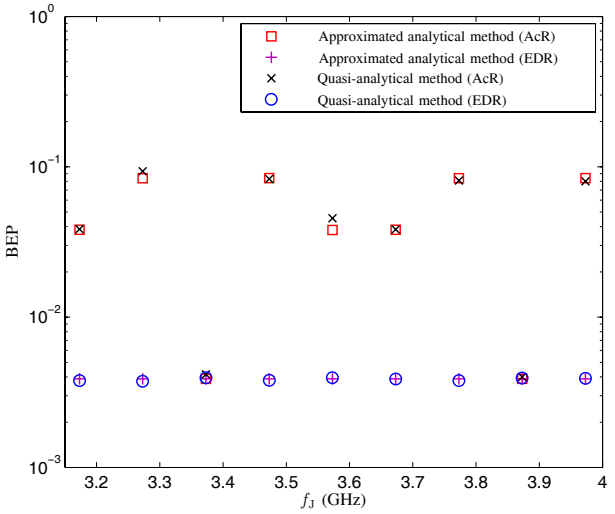

Fig. 4. BEP comparison of UWB non-coherent systems in the presence of a single NB interferer as a function of f_J for $(L, \epsilon, m) = (32, 0, 3)$, and $WT = L$.

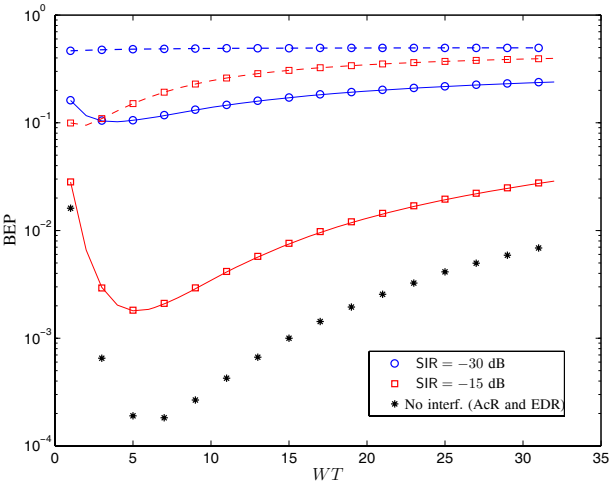

Fig. 5. BEP comparison of UWB non-coherent receiver structures in the presence of a single NB interferer for $f_J = 3.6877$ GHz, $(L, \epsilon, m) = (32, 0.4, 3)$, and $E_b/N_0 = 20$ dB. The solid and dashed lines indicate the EDR-BPPM system and AcR-TR-BPAM system, respectively.

A. Single Interferer

Figure 3 compares the BEP performance of both non-coherent receiver structures as a function of SIR in UWB channel with $(L, \epsilon, m) = (32, 0, 3)$ and $WT = L$, in the presence of a single NB interferer for $E_b/N_0 = 16, 18, 20$ dB using (33) and (40). Interestingly, we see that the performance of the AcR-TR-BPAM system strongly depends on the carrier frequency f_J of the NB interference. This is consistent with the result in [31] and it can be intuitively explained by considering that the result of a correlation between a single tone at the frequency f_J and a T_r second delayed version of it depends on the phase shift among the two signals defined by the product $f_J T_r$. On the other hand, the performance of the EDR-BPPM system is independent of f_J. This is expected since the approximate BEP expression for the EDR in (40) is independent of f_J. In addition, we observe that the EDR-based system appears to be much more robust to NB interference compared to the AcR-based system in the interference-limited regime.[18] This robustness of the EDR-BPPM system over the AcR-TR-BPAM system depends on the value of f_J as the amount of interference energy collected by the AcR varies with f_J (see (33)). However, as the NB interference becomes negligible, i.e., when SIR is greater than 5 dB, both receiver structures yield similar performance.

Figure 4 shows the validity of the approximation used in Section IV-A and IV-B. Specifically, we plot the BEP of both non-coherent receiver structures as a function of f_J with $(L, \epsilon, m) = (32, 0.4, 3)$, $WT = L$, $E_b/N_0 = 20$ dB, and SIR $= -10$ dB. We can see that the approximated analytical results obtained using (33) and (40) are in good agreement with the quasi-analytical results achieved by averaging (20) over 10000 realizations of the non-centrality parameters for AcR-TR-BPAM and EDR-BPPM, respectively, in the presence of single interferer. The realizations of the non-centrality parameters are obtained by simulating φ, $\{c_j\}$, $\{a_j\}$, $\{h_l\}$, and α_J. In addition, we observe that the two systems yield the same performance only when $f_J = n/4T_r$, where n is an odd positive integer number. This can be intuitively explained by looking at how the NB interference affects the received signal space. In the case of AcR, the "interference-cross interference" term produces a DC component, which is a function of $f_J T_r$ as shown in (32). As a result, the received signal space is no longer symmetric around zero for the case of TR signaling with BPAM. On the other hand, the symmetry of the received signal space for BPPM remains unaffected for the case of EDR.

The effect of the integration interval T on the performance

[18]Note that our analysis assumes that the NB interference bandwidth is much smaller than the reciprocal of Δ. The effect of the NB interference bandwidth on the EDR is discussed in [33] and [47].

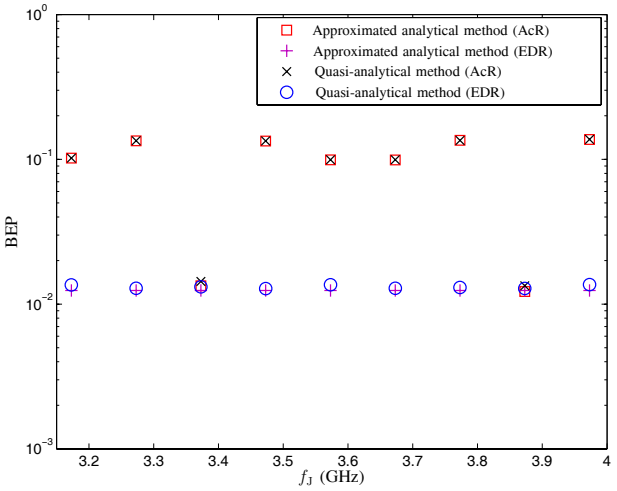

Fig. 6. BEP comparison of UWB non-coherent receiver structures in the presence of multiple NB interferers as a function of f_J for $(L, \epsilon, m) = (32, 0, 3)$, $\lambda = 0.01$ m^{-2}, $E_b/N_0 = 20$ dB, $\mathsf{SIR}_T = -10$ dB, and $WT = L$.

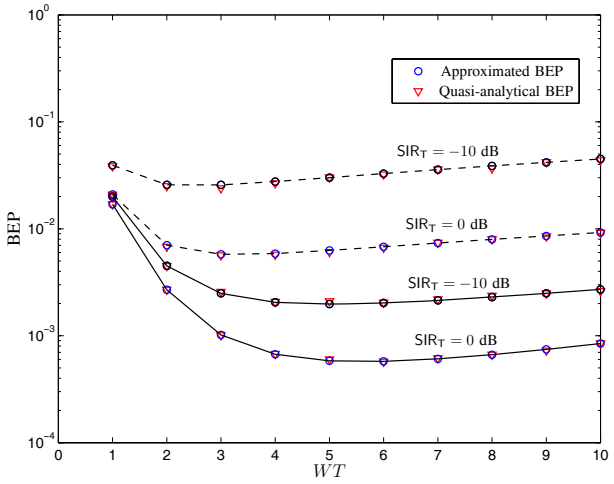

Fig. 7. BEP performance in the presence of multiple NB interferers as a function of WT for $f_J = 3.6877$ GHz, $E_b/N_0 = 20$ dB, $(L, \epsilon, m) = (32, 0.4, 3)$, $\lambda = 0.01$ m^{-2}, $\nu = 1.5$, and $\sigma_I = 1.2$ dB. Comparison between the results obtained using approximate BEP formulas (57) and (61) and, quasi-analytical BEP formulas (33) and (60) for the AcR-TR-BPAM system (dashed lines) and the EDR-BPPM system (solid lines), respectively.

of both non-coherent receiver structures in the presence of a single NB interferer at $f_J = 3.6872$ GHz with $(L, \epsilon, m) = (32, 0.4, 3)$, and $E_b/N_0 = 20$ dB is shown in Fig. 5. We can observe that there exist optimum values of T. Intuitively, the optimum integration time corresponds to the point after which the contribution of the useful signal is lower than the contribution of the interference plus noise signal. The optimum value of T is different for the two non-coherent systems. This is not surprising since the amount of interference energy accumulation for both receiver structures is different, and this amount also depends on the value of f_J for the case of AcR. Moreover, we observe that the optimum T increases with SIR, since the interference accumulation decreases with SIR. As such, it is important to appropriately design the integration interval according to the type of non-coherent receiver structure used, the operating carrier frequency of potential NB interference, the operating E_b/N_0, and the SIR.

B. Multiple Interferers

First, we show the validity of the approximate analytical method for the case of multiple NB interferers. In Fig. 6, we plot the BEP performance as a function of f_J with $(L, \epsilon, m) = (32, 0, 3)$, $\lambda = 0.01$, $WT = L$, $E_b/N_0 = 20$ dB, and $\mathsf{SIR}_T = -10$ dB for both non-coherent systems. Similar to the single NB interferer case, the approximated analytical results are in good agreement with the quasi-analytical results. The approximated analytical results were obtained by averaging the approximated conditional BEP expressions in (54) and (60) over 10,000 realizations of the chi-squared r.v. C. The quasi-analytical results were obtained by averaging (20) over 10,000 realizations of non-centrality parameters for AcR-TR-BPAM and EDR-BPPM in the presence of multiple interferers. In Fig. 7, we show the BEP performance of both non-coherent receiver structures as a function of WT with $E_b/N_0 = 20$ dB, $f_J = 3.6877$ GHz, $(L, \epsilon, m) = (32, 0.4, 3)$, $\lambda = 0.01$ m^{-2}, $\nu = 1.5$, and $\sigma_I = 1.2$ dB. We observe that the approximated analytical results obtained using (57) and (61) are in good

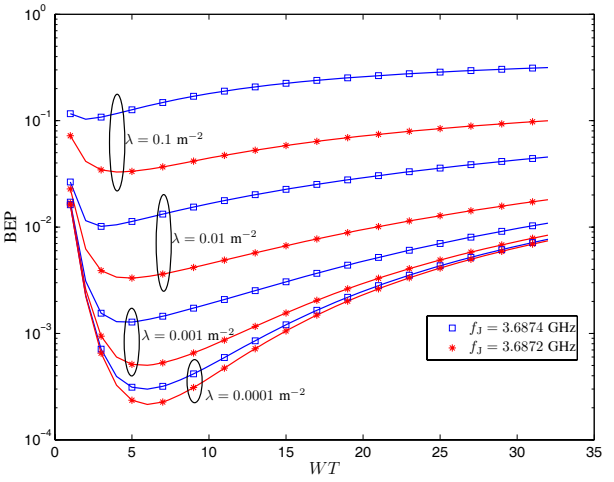

Fig. 8. Effect of the multiple NB interferers spatial density λ and of the NB interference carrier frequency f_J on the optimum integration time of the AcR-TR-BPAM system for $E_b/N_0 = 20$ dB, $\mathsf{SIR}_T = -10$ dB, $(L, \epsilon, m) = (32, 0.4, 3)$, $\nu = 1.5$, and $\sigma_I = 1.2$ dB.

agreement with quasi-analytical results obtained by averaging (54) and (60) over several realization of the r.v. C. Thus, the approximated BEP expressions in (57) and (61) are useful for investigating the performance of AcR and EDR in the presence of multiple NB interferers. As in the case of a single NB interferer, the EDR-based system performs better than the AcR-based system. We also observe that the optimum T for both receiver structures are different,

Next, we investigate the effect of spatial density λ of the multiple NB interferers on the optimum integration interval T of AcR-TR-BPAM and EDR-BPPM systems with $E_b/N_0 = 20$ dB, $(L, \epsilon, m) = (32, 0.4, 3)$, $\nu = 1.5$, and $\sigma_I = 1.2$ dB in Fig. 8 and 9, respectively. As λ increases, the aggregate NB interference becomes stronger and consequently, the optimum integration interval needs to be smaller to reduce the amount

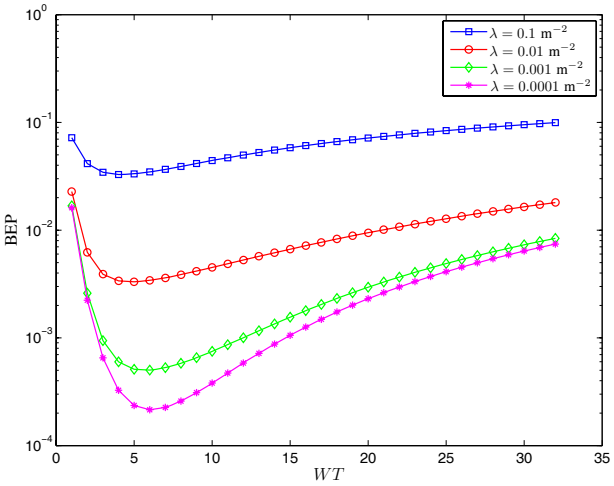

Fig. 9. Effect of the multiple NB interferers spatial density λ on the optimum integration time of EDR-BPPM system for $E_{\rm b}/N_0 = 20$ dB, $\mathsf{SIR}_{\rm T} = -10$ dB, $(L, \epsilon, m) = (32, 0.4, 3)$, $\nu = 1.5$, and $\sigma_{\rm I} = 1.2$ dB.

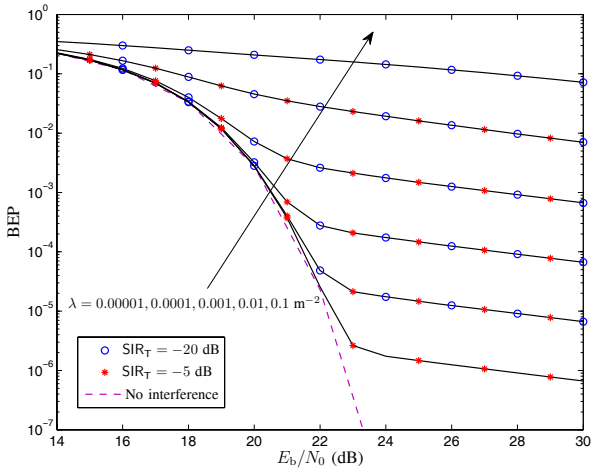

Fig. 10. Combined effect of the parameters λ and $\mathsf{SIR}_{\rm T}$ on the BEP performance of the EDR-BPPM system for $(L, \epsilon, m) = (32, 0, 3)$, $WT = L$, $\nu = 1.5$, and $\sigma_{\rm I} = 1.2$ dB.

of interference energy accumulation. Similar to the single NB interferer results, we see that the performance of AcR-based system strongly depends on the NB interference carrier frequency.

Lastly, we illustrate how our results can be useful for coexistence planning between UWB systems and multiple NB interferers systems. Specifically, we plot in Fig. 10 the BEP performance of EDR-BPPM system as a function of $E_{\rm b}/N_0$ for $(L, \epsilon, m) = (32, 0, 3)$, $WT = L$, $\nu = 1.5$, and $\sigma_{\rm I} = 1.2$ dB. We see that a reduction of 10 dB in the spatial density of the interferers allows the increase of the individual interferer power by 15 dB. The relationship between the reduction of the spatial density Δ_λ^- and the increase of the individual interferer power $\Delta_{\rm I}^+$, both expressed in dB, can be derived from (60) and (52), where $\Delta_{\rm I}^+ = \nu\Delta_\lambda^-$. Note that we will use (57) instead of (61) for the case of AcR-based system.

VII. Conclusion

In this paper, we compared two non-coherent UWB receiver structures in terms of BEP performance in multipath fading channels both in the absence and presence of NB interference. In the absence of NB interference, we showed the equivalence of these two receiver structures in terms of their BEP performance under certain conditions on pulse energy and signaling structure. On the other hand, when NB interference is present, we showed that the EDR-based system is more robust than the AcR-based system. We considered both single and multiple NB interferers cases. In the multiple NB interferers case, we considered that the interfering nodes are scattered according to a spatial Poisson process and showed that the aggregate interference can be represented by a single tone NB interference with a CS complex stable r.v.. Our framework is simple enough to enable a tractable analysis and can serve as a guideline for the design of heterogeneous networks where coexistence between UWB and NB systems is of importance. There are many important extensions to this paper that are worth pursuing. For example, one possible direction is to generalize the formulation to the case where the interfering nodes are operated on different carrier frequencies. The coexistence between uncoordinated networks, where multiple wideband interferer are present, is also an interesting issue to be investigated . Some work in this direction can be found in [47], [48].

VIII. Acknowledgments

The authors would like to thank M. Chiani, D. Dardari, W. M. Gifford, A. Giorgetti, and W. Suwansantisuk for their helpful suggestions.

Appendix A
Derivation of the Distribution of $\mathbf{A}$

If a homogeneous Poisson point process in the plane has spatial density λ and R_n denotes the distance of node i to the origin, then, by the mapping theorem [39], the sequence $\{R_n^2\}_{n=1}^{\infty}$ represents Poisson arrival times on the line with constant arrival rate $\lambda\pi$. Using this fact, it can be shown that $\mathbf{A}$ in (45) has the following distribution [46], [49]

$$\mathbf{A} = \sum_{n=1}^{\infty} \frac{e^{\sigma_{\rm I} G_n}\mathbf{X}_n}{R_n^{\nu}} \overset{\text{a.s.}}{\sim} \mathcal{S}_{\rm c}\left(\alpha = \frac{2}{\nu},\ \beta = 0,\ \gamma = \lambda\pi C_{2/\nu}^{-1}\mathbb{E}\{|e^{\sigma_{\rm I} G_n} X_{n,j}|^{2/\nu}\}\right) \tag{62}$$

for $\nu > 1$, which simplifies to (46). Note that $\mathbf{X}_n$ is CS due to the uniform phase ϕ_n, implying that $\mathbf{A}$ is CS. Thus $\mathbf{A}$ can be decomposed as follows [46]:

$$\mathbf{A} = \sqrt{V}\mathbf{G} \tag{63}$$

with $V \sim \mathcal{S}(\alpha/2, 1, \cos(\frac{\pi\alpha}{4}))$ and $\mathbf{G} = G_1 + \jmath G_2$, where G_1 and G_2 are i.i.d Gaussian r.v.'s with zero mean and variance $2\gamma^{2/\alpha}$, respectively. In addition, V and $\mathbf{G}$ are independent.

APPENDIX B
DERIVATION OF $\mu_{\mathrm{TR},Y_1}^{(\mathrm{NBIs})}$ AND $\mu_{\mathrm{TR},Y_2}^{(\mathrm{NBIs})}$

The non-centrality parameter of $Y_{\mathrm{TR},1}$ is defined as

$$\mu_{Y_{\mathrm{TR},1}}^{(\mathrm{NBIs})} \triangleq \underbrace{\frac{1}{2\sigma_{\mathrm{TR}}^2}\int_0^T w_j^2(t)dt}_{\triangleq \mu_{\mathrm{A,TR}}} + \underbrace{\frac{1}{2\sigma_{\mathrm{TR}}^2}\int_0^T \frac{\left(\zeta_{1,j}(t)+\zeta_{2,j}(t)\right)^2}{4}dt}_{\triangleq \mu_{\mathrm{B,TR}}^{(\mathrm{NBIs})}} + \underbrace{\frac{1}{2\sigma_{\mathrm{TR}}^2}\int_0^T w_j(t)\left[\zeta_{1,j}(t)+\zeta_{2,j}(t)\right]dt}_{\triangleq \mu_{\mathrm{C,TR}}^{(\mathrm{NBIs})}}. \quad (64)$$

The term $\mu_{\mathrm{A,TR}}$ is the same as that in (29) defined for the case of single NB interferer. The term $\mu_{\mathrm{B,TR}}^{(\mathrm{NBIs})}$ can be derived by expanding all the terms as shown in (65), (66), and (67) at the top of next page.

The approximations in (65) are obtained considering that $T \gg \frac{1}{4\pi f_{\mathrm{J}}}$, $|\sin\phi| \leq 1$, $|\cos\phi| \leq 1$ and $|\mathbf{A}|^2 \geq |A_{\mathrm{c}}A_{\mathrm{s}}|$. In addition, $\mu_{\mathrm{D,TR}}^{(\mathrm{NBIs})} = \frac{|\mathbf{A}|^2 ITN_{\mathrm{s}}}{2N_0}\cos\left(2\pi f_{\mathrm{J}}T_{\mathrm{r}}\right)$ when $T\cos\left(2\pi f_{\mathrm{J}}T_{\mathrm{r}}\right) \gg \frac{1}{4\pi f_{\mathrm{J}}}$. Otherwise, $\mu_{\mathrm{D,TR}}^{(\mathrm{NBIs})}$ is of the same order as $\frac{1}{4\pi f_{\mathrm{J}}}$, which is negligible compared to the first term of $\mu_{\mathrm{B,TR}}^{(\mathrm{NBIs})}$. As a result we can ignore the latter case and consider only the scenario when $T\cos\left(2\pi f_{\mathrm{J}}T_{\mathrm{r}}\right) \gg \frac{1}{4\pi f_{\mathrm{J}}}$. The term $\mu_{\mathrm{B,TR}}^{(\mathrm{NBIs})}$ can then be approximated as

$$\mu_{\mathrm{B,TR}}^{(\mathrm{NBIs})} \approx \frac{|\mathbf{A}|^2 ITN_{\mathrm{s}}}{2N_0}\Big[1+\cos\left(2\pi f_{\mathrm{J}}T_{\mathrm{r}}\right)\Big]. \quad (68)$$

The third term $\mu_{\mathrm{C,TR}}^{(\mathrm{NBIs})}$ can be derived as shown in (69) at the top of this page. Substituting the expressions of $\mu_{\mathrm{A,TR}}$, $\mu_{\mathrm{B,TR}}^{(\mathrm{NBIs})}$, and $\mu_{\mathrm{C,TR}}^{(\mathrm{NBIs})}$ in (64), we obtain (48).

Using a similar approach leading to (68), the non-centrality parameter of $Y_{\mathrm{TR},2}$ be approximated as follows:

$$Y_{\mathrm{TR},2} \approx \frac{|\mathbf{A}|^2 ITN_{\mathrm{s}}}{2N_0}\Big[1-\cos\left(2\pi f_{\mathrm{J}}T_{\mathrm{r}}\right)\Big]. \quad (70)$$

REFERENCES

[1] M. Z. Win and R. A. Scholtz, "Impulse radio: how it works," *IEEE Commun. Lett.*, vol. 2, no. 2, pp. 36–38, Feb. 1998.

[2] ——, "Ultra-wide bandwidth time-hopping spread-spectrum impulse radio for wireless multiple-access communications," *IEEE Trans. Commun.*, vol. 48, no. 4, pp. 679–691, Apr. 2000.

[3] L. Yang and G. B. Giannakis, "Ultra-wideband communications: an idea whose time has come," *IEEE Signal Process. Mag.*, vol. 21, no. 6, pp. 26–54, Nov. 2004.

[4] S. Gezici, Z. Tian, G. B. Giannakis, H. Kobayashi, A. F. Molisch, H. V. Poor, and Z. Sahinoglu, "Localization via ultra-wideband radios: a look at positioning aspects of future sensor networks," *IEEE Signal Process. Mag.*, vol. 22, no. 4, pp. 70–84, July 2005.

[5] D. Dardari, A. Conti, U. J. Ferner, A. Giorgetti, and M. Z. Win, "Ranging with ultrawide bandwidth signals in multipath environments," *Proc. IEEE*, vol. 97, no. 2, pp. 404–426, Feb. 2009.

[6] S. Gezici and H. V. Poor, "Position estimation via ultra-wide-band signals," *Proc. IEEE*, vol. 97, no. 2, pp. 386–403, Feb. 2009.

[7] Y. Shen and M. Z. Win, "Fundamental limits of wideband localization–part I: a general framework," *IEEE Trans. Inf. Theory*, vol. 56, vol. 56, no. 10, Oct. 2010.

[8] Y. Shen, H. Wymeersch, and M. Z. Win, "Fundamental limits of wideband localization–part II: cooperative networks," *IEEE Trans. Inf. Theory*, vol. 56, no. 10, Oct. 2010.

[9] B. Denis, J.-B. Pierrot, and C. Abou-Rjeily, "Joint distributed synchronization and positioning in UWB ad hoc networks using TOA," *IEEE Trans. Microw. Theory Tech.*, vol. 54, no. 4, pp. 1896–1911, Apr. 2006.

[10] N. A. Alsindi, B. Alavi, and K. Pahlavan, "Measurement and modeling of ultrawideband TOA-based ranging in indoor multipath environments," *IEEE Trans. Veh. Technol.*, vol. 58, no. 3, pp. 1046–1058, Mar. 2009.

[11] M. Z. Win and R. A. Scholtz, "On the robustness of ultra-wide bandwidth signals in dense multipath environments," *IEEE Commun. Lett.*, vol. 2, no. 2, pp. 51–53, Feb. 1998.

[12] M. Z. Win and R. A. Scholtz, "Characterization of ultra-wide bandwidth wireless indoor communications channel: a communication theoretic view," *IEEE J. Sel. Areas Commun.*, vol. 20, no. 9, pp. 1613–1627, Dec. 2002.

[13] A. A. D'Amico, U. Mengali, and L. Taponecco, "Impact of MAI and channel estimation errors on the performance of Rake receivers in UWB communications," *IEEE Trans. Wireless Commun.*, vol. 4, no. 5, pp. 2435–2440, Sep. 2005.

[14] D. Cassioli, M. Z. Win, and A. F. Molisch, "The ultra-wide bandwidth indoor channel: from statistical model to simulations," *IEEE J. Sel. Areas Commun.*, vol. 20, no. 6, pp. 1247–1257, Aug. 2002.

[15] A. F. Molisch, "Ultrawideband propagation channels-theory, measurements, and modeling," *IEEE Trans. Veh. Technol.*, vol. 54, no. 5, pp. 1528–1545, Sep. 2005.

[16] ——, "Ultra-wide-band propagation channels," *Proc. IEEE*, vol. 97, no. 2, pp. 353–371, Feb. 2009.

[17] M. Z. Win, "A unified spectral analysis of generalized time-hopping spread-spectrum signals in the presence of timing jitter," *IEEE J. Sel. Areas Commun.*, vol. 20, no. 9, pp. 1664–1676, Dec. 2002.

[18] L. Zhao and A. M. Haimovich, "Performance of ultra-wideband communications in the presence of interference," *IEEE J. Sel. Areas Commun.*, vol. 20, no. 9, pp. 1684–1691, Dec. 2002.

[19] M. Chiani and A. Giorgetti, "Coexistence between UWB and narrowband wireless communication systems," *Proc. IEEE*, vol. 97, no. 2, pp. 231–254, Feb. 2009.

[20] "P802.15.4a-2007, PART 15.4: wireless medium access control (MAC) and physical layer (PHY) specifications for low-rate wireless personal area networks (LR-WPANs): amendment to add alternate PHY (amendment of IEEE std 802.15.4)," 2007.

[21] J. Zhang, P. V. Orlik, Z. Sahinoglu, A. F. Molisch, and P. Kinney, "UWB systems for wireless sensor networks," *Proc. IEEE*, vol. 97, no. 2, pp. 313–331, Feb. 2009.

[22] J. D. Choi and W. E. Stark, "Performance of ultra-wideband communications with suboptimal receivers in multipath channels," *IEEE J. Sel. Areas Commun.*, vol. 20, no. 9, pp. 1754–1766, Dec. 2002.

[23] L. Yang and G. B. Giannakis, "Optimal pilot waveform assisted modulation for ultrawideband communications," *IEEE Trans. Wireless Commun.*, vol. 3, no. 4, pp. 1236–1249, July 2004.

[24] A. A. D'Amico and U. Mengali, "GLRT receivers for UWB systems," *IEEE Commun. Lett.*, vol. 9, no. 6, pp. 487–489, June 2005.

[25] S. Franz and U. Mitra, "Generalized UWB transmitted reference systems," *IEEE J. Sel. Areas Commun.*, vol. 24, no. 4, pp. 780–786, Apr. 2006.

[26] G. D. Hingorani, "Error rates for a class of binary receivers," *IEEE Trans. Commun. Technol.*, vol. 15, no. 2, pp. 209–215, Apr. 1967.

[27] T. Q. S. Quek and M. Z. Win, "Analysis of UWB transmitted-reference communication systems in dense multipath channels," *IEEE J. Sel. Areas Commun.*, vol. 23, no. 9, pp. 1863–1874, Sep. 2005.

[28] R. Hoctor and H. Tomlinson, "Delay-hopped transmitted-reference RF communications," in *Proc. IEEE Conf. Ultra Wideband Systems and Technologies*, Baltimore, MD, May 2002, pp. 265-270.

[29] M. Pausini and G. Janssen, "On the narrowband interference in transmitted reference UWB receivers," in *Proc. IEEE Int. Conf. on Ultra-Wideband*, Zurich, Switzerland, Sep. 2005, pp. 571–575.

[30] Y. Alemseged and K. Witrisal, "Modeling and mitigation of narrowband interference for transmitted-reference UWB systems," *IEEE J. Sel. Topics Signal Process.*, vol. 1, no. 3, pp. 456–469, Oct. 2007.

[31] T. Q. S. Quek, M. Z. Win, and D. Dardari, "Unified analysis of UWB transmitted-reference schemes in the presence of narrowband interference," *IEEE Trans. Wireless Commun.*, vol. 6, no. 6, pp. 2126–2139, June 2007.

[32] M. Weisenhorn and W. Hirt, "Robust noncoherent receiver exploiting UWB channel properties," in *Proc. IEEE Conf. Ultra Wideband Systems and Technologies*, Kyoto, Japan, May 2004, pp. 156–160.

$$\frac{1}{2N_0}\sum_{j=0}^{\frac{N_\mathrm{s}}{2}-1}\int_0^T \zeta_{1,j}^2(t)dt = \frac{A_\mathrm{c}^2 I}{2N_0}\sum_{j=0}^{\frac{N_\mathrm{s}}{2}-1}\left[T+\frac{\sin\left(4\pi f_\mathrm{J}(T+j2T_\mathrm{f}^\mathrm{TR}+c_jT_\mathrm{p})\right)}{4\pi f_\mathrm{J}}-\frac{\sin\left(4\pi f_\mathrm{J}(j2T_\mathrm{f}^\mathrm{TR}+c_jT_\mathrm{p})\right)}{4\pi f_\mathrm{J}}\right]$$
$$+\frac{A_\mathrm{c}A_\mathrm{s}I}{N_0}\sum_{j=0}^{\frac{N_\mathrm{s}}{2}-1}\left[\frac{\cos\left(4\pi f_\mathrm{J}\left(T+j2T_\mathrm{f}^\mathrm{TR}+c_jT_\mathrm{p}\right)\right)}{4\pi f_\mathrm{J}}-\frac{\cos\left(4\pi f_\mathrm{J}\left(j2T_\mathrm{f}^\mathrm{TR}+c_jT_\mathrm{p}\right)\right)}{4\pi f_\mathrm{J}}\right]$$
$$+\frac{A_\mathrm{s}^2 I}{2N_0}\sum_{j=0}^{\frac{N_\mathrm{s}}{2}-1}\left[T-\frac{\sin\left(4\pi f_\mathrm{J}(T+j2T_\mathrm{f}^\mathrm{TR}+c_jT_\mathrm{p})\right)}{4\pi f_\mathrm{J}}+\frac{\sin\left(4\pi f_\mathrm{J}(j2T_\mathrm{f}^\mathrm{TR}+c_jT_\mathrm{p})\right)}{4\pi f_\mathrm{J}}\right]$$
$$\approx \frac{|\mathbf{A}|^2 ITN_\mathrm{s}}{4N_0}, \tag{65}$$

$$\frac{1}{2N_0}\sum_{j=0}^{\frac{N_\mathrm{s}}{2}-1}\int_0^T \zeta_{2,j}^2(t)dt \approx \frac{|\mathbf{A}|^2 ITN_\mathrm{s}}{4N_0}, \tag{66}$$

$$\frac{1}{N_0}\sum_{j=0}^{\frac{N_\mathrm{s}}{2}-1}\int_0^T \zeta_{1,j}(t)\zeta_{2,j}(t)dt \approx \mu_{\mathrm{D,TR}}^{(\mathrm{NBIs})}. \tag{67}$$

$$\mu_{\mathrm{C,TR}}^{(\mathrm{NBIs})} = \frac{2\sqrt{2E_\mathrm{p}^\mathrm{TR}I}A_\mathrm{C}}{N_0}\sum_{j=0}^{\frac{N_\mathrm{s}}{2}-1}a_j\sum_{l=1}^{L_\mathrm{CAP}}h_l\int_0^{T_\mathrm{p}}p(t)\left[\cos\left(2\pi f_\mathrm{J}(t+\tau_l+j2T_\mathrm{f}^\mathrm{TR}+c_jT_\mathrm{p})\right)\right.$$
$$\left.+\cos\left(2\pi f_\mathrm{J}(t+\tau_l+j2T_\mathrm{f}^\mathrm{TR}+c_jT_\mathrm{p}+T_\mathrm{r})\right)\right]dt$$
$$-\frac{2\sqrt{2E_\mathrm{p}^\mathrm{TR}I}A_\mathrm{s}}{N_0}\sum_{j=0}^{\frac{N_\mathrm{s}}{2}-1}a_j\sum_{l=1}^{L_\mathrm{CAP}}h_l\int_0^{T_\mathrm{p}}p(t)\left[\sin\left(2\pi f_\mathrm{J}(t+\tau_l+j2T_\mathrm{f}^\mathrm{TR}+c_jT_\mathrm{p})\right)\right.$$
$$\left.+\sin\left(2\pi f_\mathrm{J}(t+\tau_l+j2T_\mathrm{f}^\mathrm{TR}+c_jT_\mathrm{p}+T_\mathrm{r})\right)\right]dt$$
$$=\frac{4|\widehat{P}(f_\mathrm{J})|\sqrt{2E_\mathrm{p}^\mathrm{TR}I}}{N_0}\sum_{j=0}^{\frac{N_\mathrm{s}}{2}-1}a_j\sum_{l=1}^{L_\mathrm{CAP}}h_l\left[A_\mathrm{c}\cos\left(\pi f_\mathrm{J}T_\mathrm{r}\right)\cos\left(2\pi f_\mathrm{J}\left(\tau_l+j2T_\mathrm{f}^\mathrm{TR}+c_jT_\mathrm{p}+T_\mathrm{r}/2\right)+\tilde{\varphi}\right)\right.$$
$$\left.-A_\mathrm{s}\cos\left(\pi f_\mathrm{J}T_\mathrm{r}\right)\sin\left(2\pi f_\mathrm{J}\left(\tau_l+j2T_\mathrm{f}^\mathrm{TR}+c_jT_\mathrm{p}+T_\mathrm{r}/2\right)+\tilde{\varphi}\right)\right]. \tag{69}$$

[33] C. Steiner and A. Wittneben, "On the interference robustness of ultra-wideband energy detection receivers," in *Proc. IEEE Int. Conf. on Ultra-Wideband*, Singapore, Sep. 2007, pp. 721–726.

[34] M. Z. Win, P. C. Pinto, and L. A. Shepp, "A mathematical theory of network interference and its applications," *Proc. IEEE*, vol. 97, no. 2, pp. 205–230, Feb. 2009.

[35] P. C. Pinto, A. Giorgetti, M. Z. Win, and M. Chiani, "A stochastic geometry approach to coexistence in heterogeneous wireless networks," *IEEE J. Sel. Areas Commun.*, vol. 27, no. 7, pp. 1268–1282, Sep. 2009.

[36] E. Sousa, "Performance of a spread spectrum packet radio network link in a Poisson field of interferers," *IEEE Trans. Inf. Theory*, vol. 38, no. 6, pp. 1743–1754, 1992.

[37] J. Ilow, D. Hatzinakos, and A. Venetsanopoulos, "Performance of FH SS radio networks with interference modeled as a mixture of Gaussian and alpha-stable noise," *IEEE Trans. Commun.*, vol. 46, no. 4, pp. 509–520, 1998.

[38] M. Haenggi, J. G. Andrews, F. Baccelli, O. Dousse, and M. Franceschetti, "Stochastic geometry and random graphs for the analysis and design of wireless networks," *IEEE J. Sel. Areas Commun.*, vol. 27, no. 7, pp. 1029–1046, Sep. 2009.

[39] J. Kingman, *Poisson Processes*. Oxford University Press, 1993.

[40] A. Giorgetti, M. Chiani, and M. Z. Win, "The effect of narrowband interference on wideband wireless communication systems," *IEEE Trans. Commun.*, vol. 53, no. 12, pp. 2139–2149, Dec. 2005.

[41] W. C. Jakes, Ed., *Microwave Mobile Communications*, classic reissue edition. Piscataway, NJ: IEEE Press, 1995.

[42] A. F. Molisch, *Wireless Communications*. IEEE Press, J. Wiley and Sons, 2005.

[43] A. Goldsmith, *Wireless Communications*. Cambridge University Press, 2005.

[44] M. K. Simon and M.-S. Alouini, *Digital Communication over Fading Channels: A Unified Approach to Performance Analysis*, 1st edition. New York: John Wiley & Sons, Inc., 2000.

[45] J. Gil-Pelaez, "Note on the inversion theorem," *Biometrika*, vol. 38, no. 3/4, pp. 481–482, Dec. 1951.

[46] G. Samoradnitsky and M. Taqqu, *Stable Non-Gaussian Random Processes*. Chapman and Hall, 1994.

[47] A. Rabbachin, T. Q. S. Quek, I. Oppermann, and M. Z. Win, "Effect of uncoordinated network interference on UWB energy detection receiver," in *Proc. IEEE Workshop on Signal Process. Advances in Wireless Commun.*, Perugia, Italy, June 2009, pp. 692–696.

[48] ——, "Effect of uncoordinated network interference on UWB autocorrelation receiver," in *Proc. IEEE Int. Conf. on Ultra-Wideband*, Vancouver, Canada, Sep. 2009, pp. 65–70.

[49] P. C. Pinto and M. Z. Win, "Communication in a Poisson field of interferers–part I: interference distribution and error probability," *IEEE Trans. Wireless Commun.*, vol. 9, no. 7, pp. 2176-2186, Jul. 2010.

Alberto Rabbachin (S'03–M'07) received the M.S. degree from the University of Bologna (Italy) in 2001 and the Ph.D. degree from the University of Oulu (Finland) in 2008. Since 2008 he is a Postdoctoral researcher with the Institute for the Protection and Security of the Citizen of the European Commission Joint Research Center. He has done research on ultrawideband (UWB) impulse-radio techniques, with emphasis on receiver architectures, synchronization, and ranging algorithms, as well as on low-complexity UWB transceiver design. He is the author of several book chapters, international journal papers, conference proceedings, and international standard contributions. His current research interests include aggregate interference statistical modeling, cognitive radio, and wireless body area networks. Dr. Rabbachin received the Nokia Fellowship for year 2005 and 2006, and the IEEE Globecom 2010 Best Paper Award. He has served on the Technical Program Committees of various international conferences.

Tony Q.S. Quek (S'98–M'08) received the B.E. and M.E. degrees in Electrical and Electronics Engineering from Tokyo Institute of Technology, Tokyo, Japan, in 1998 and 2000, respectively. At Massachusetts Institute of Technology (MIT), Cambridge, MA, he earned the Ph.D. in Electrical Engineering and Computer Science in Feb. 2008.

From 2001 to 2002, he was with the Centre for Wireless Communications, Singapore, as a Research Engineer. Since 2008, he has been with the Institute for Infocomm Research, A*STAR, where he is currently a Principal Investigator and Senior Research Engineer. He is also an Adjunct Assistant Professor with the Division of Communication Engineering, Nanyang Technological University. His main research interests are the application of mathematical, optimization, and statistical theories to communication, detection, information theoretic and resource allocation problems. Specific current research topics include cooperative networks, interference networks, heterogeneous networks, green communications, wireless security, and cognitive radio.

Dr. Quek has been actively involved in organizing and chairing sessions, and has served as a member of the Technical Program Committee (TPC) in a number of international conferences. He served as the Technical Program Chair for the Services & Applications Track for the IEEE Wireless Communications and Networking Conference (WCNC) in 2009 and the Cognitive Radio & Cooperative Communications Track for the IEEE Vehicular Technology Conference (VTC) in Spring 2011; as Technical Program Vice-Chair for the IEEE Conference on Ultra Wideband in 2011; and as the Workshop Chair for the IEEE Globecom 2010 Workshop on Femtocell Networks and the IEEE ICC 2011 Workshop on Heterogeneous Networks. Dr. Quek is currently an Editor for *Wiley Journal on Security and Communication Networks*. He was Guest Editor for the *Journal of Communications and Networks* (Special Issue on Heterogeneous Networks) in 2011.

Dr. Quek received the Singapore Government Scholarship in 1993, Tokyu Foundation Fellowship in 1998, and the A*STAR National Science Scholarship in 2002. He was honored with the 2008 Philip Yeo Prize for Outstanding Achievement in Research from the A*STAR Science and Engineering Research Council and the IEEE Globecom 2010 Best Paper Award.

Pedro C. Pinto (S'04) received the Licenciatura degree with highest honors in Electrical and Computer Engineering from the University of Porto, Portugal, in 2003. He received the M.S. degree in Electrical Engineering and Computer Science from the Massachusetts Institute of Technology (MIT) in 2006. Since 2004, he has been with the MIT Laboratory for Information and Decision Systems (LIDS), where he is now a Ph.D. candidate. His main research interests are in wireless communications and signal processing. He was the recipient of the MIT Claude E. Shannon Fellowship in 2007, the Best Student Paper Award at the IEEE International Conference on Ultra-Wideband in 2006, and the Infineon Technologies Award in 2003.

Ian Oppermann (SM'02) Dr. Ian Oppermann is currently the Director of CSIROs ICT Centre. Prior to joining CSIRO, Ian was the Head of Sales Partnering at Nokia Siemens Networks responsible for new business development with Technology and Sales Partners for the software business unit. Before joining Nokia, he was the Director of the Centre for Wireless Communications (CWC), a self funded research centre in Oulu, Finland. At the CWC, Ian was responsible for looking at "beyond 3G" systems with a focus on ad-hoc networks.

Ian holds undergraduate degrees in Science (1990) and Electrical Engineering (1992) from the University of Sydney, Australia. He also earned his Ph.D. from the University of Sydney in 1997 where his thesis explored CDMA physical layer technologies. In 2005, he completed an MBA at the University of London.

Moe Z. Win (S'85-M'87-SM'97-F'04) received both the Ph.D. in Electrical Engineering and M.S. in Applied Mathematics as a Presidential Fellow at the University of Southern California (USC) in 1998. He received an M.S. in Electrical Engineering from USC in 1989, and a B.S. (*magna cum laude*) in Electrical Engineering from Texas A&M University in 1987.

Dr. Win is an Associate Professor at the Massachusetts Institute of Technology (MIT). Prior to joining MIT, he was at AT&T Research Laboratories for five years and at the Jet Propulsion Laboratory for seven years. His research encompasses developing fundamental theories, designing algorithms, and conducting experimentation for a broad range of real-world problems. His current research topics include location-aware networks, intrinsically secure wireless networks, aggregate interference in heterogeneous networks, ultra-wide bandwidth systems, multiple antenna systems, time-varying channels, optical transmission systems, and space communications systems.

Professor Win is an IEEE Distinguished Lecturer and elected Fellow of the IEEE, cited for "contributions to wideband wireless transmission." He was honored with the IEEE Eric E. Sumner Award (2006), an IEEE Technical Field Award for "pioneering contributions to ultra-wide band communications science and technology." Together with students and colleagues, his papers have received several awards including the IEEE Communications Society's Guglielmo Marconi Best Paper Award (2008) and the IEEE Antennas and Propagation Society's Sergei A. Schelkunoff Transactions Prize Paper Award (2003). His other recognitions include the Laurea Honoris Causa from the University of Ferrara, Italy (2008), the Technical Recognition Award of the IEEE ComSoc Radio Communications Committee (2008), Wireless Educator of the Year Award (2007), the Fulbright Foundation Senior Scholar Lecturing and Research Fellowship (2004), the U.S. Presidential Early Career Award for Scientists and Engineers (2004), the AIAA Young Aerospace Engineer of the Year (2004), and the Office of Naval Research Young Investigator Award (2003).

Professor Win has been actively involved in organizing and chairing a number of international conferences. He served as the Technical Program Chair for the IEEE Wireless Communications and Networking Conference in 2009, the IEEE Conference on Ultra Wideband in 2006, the IEEE Communication Theory Symposia of ICC-2004 and Globecom-2000, and the IEEE Conference on Ultra Wideband Systems and Technologies in 2002; Technical Program Vice-Chair for the IEEE International Conference on Communications in 2002; and the Tutorial Chair for ICC-2009 and the IEEE Semiannual International Vehicular Technology Conference in Fall 2001. He was the chair (2004-2006) and secretary (2002-2004) for the Radio Communications Committee of the IEEE Communications Society. Dr. Win is currently an Editor for IEEE TRANSACTIONS ON WIRELESS COMMUNICATIONS. He served as Area Editor for *Modulation and Signal Design* (2003-2006), Editor for *Wideband Wireless and Diversity* (2003-2006), and Editor for *Equalization and Diversity* (1998-2003), all for the IEEE TRANSACTIONS ON COMMUNICATIONS. He was Guest-Editor for the PROCEEDINGS OF THE IEEE (Special Issue on UWB Technology & Emerging Applications) in 2009 and IEEE JOURNAL ON SELECTED AREAS IN COMMUNICATIONS (Special Issue on Ultra -Wideband Radio in Multiaccess Wireless Communications) in 2002.